Final Report 1998-19

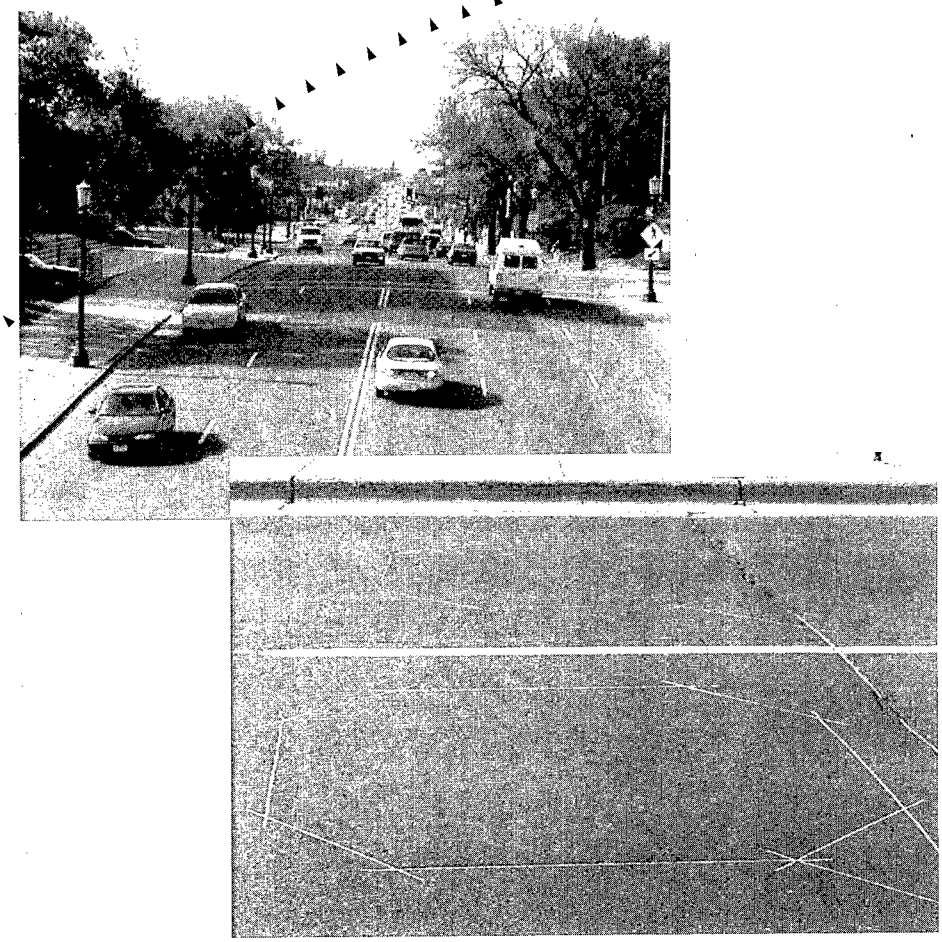

Estimating Arterial Travel Time Using Loop Data - Phase II

Technical Report Documentation Page

1. Report No.	2.	PB99-112013
MN/RC - 98/19		

4. Title and Subtitle	5. Report Date
ESTIMATING ARTERIAL TRAVEL TIME USING LOOP DATA - Phase II	August 1998
	6.

7. Author(s)	8. Performing Organization Report No.
Michael Zhang, Eil Kwon, Tong Qiang Wu, Kevin Sommers, Ahsan Habib	

9. Performing Organization Name and Address	10. Project/Task/Work Unit No.
Department of Civil & Environmental Engineering and Public Policy Center University of Iowa Iowa City, Iowa 52242-1192	11. Contract (C) or Grant (G) No. (C) 74884 TOC # 2

12. Sponsoring Organization Name and Address	13. Type of Report and Period Covered
Minnesota Department of Transportation 395 John Ireland Boulevard Mail Stop 330 St. Paul, Minnesota 55155	Final Report 1997-1998
	14. Sponsoring Agency Code

15. Supplementary Notes

16. Abstract (Limit: 200 words)

Successful implementation of advanced traveler information systems over an entire urban network requires real-time measurement or estimation of arterial travel times (or equivalently arterial journey speeds). This project develops an arterial journey speed model using data from inductive loop detectors and traffic controllers.

This model incorporates the following key findings of traffic data analysis that researchers collected in Phase I.
- Spot speeds are highly correlated with journey speeds when both speeds are low (0-15 mph) and uncorrelated with journey speeds when both speeds are high (greater than 25 mph).
- Signal offsets or greenband width, traffic demand, green splits and capacity-reduction incidents are major factors that affect arterial travel time/journey speed.

The model consists of two parts--the speed estimated from the volume and occupancy measured by detectors and the speed estimated based on critical volume/capacity ratio. Researchers tested and compared the model with a number of existing models, with promising results.

17. Document Analysis/Descriptors	18. Availability Statement
travel time detector arterial traffic	No restrictions. Document available from: National Technical Information Services, Springfield, Virginia 22161

19. Security Class (this report)	20. Security Class (this page)	21. No. of Pages	22. Price
Unclassified	Unclassified	85	

ESTIMATING ARTERIAL TRAVEL TIME USING LOOP DATA - Phase II

Final Report

Prepared by:

H.M. Zhang, Assistant Professor
J.C. He, Graduate Research Assistant
Department of Civil and Environmental Engineering
and Public Policy Center
The University of Iowa
Iowa City, Iowa 52242

May 1998

Published by:

Minnesota Department of Transportation
Office of Research Services
Mail Stop 330
395 John Ireland Boulevard
St. Paul, MN 55155

Acknowledgments:

We would like to thank Mr. Ray Starr, Metro Division, Minnesota Department of Transportation for the support and guidance he provided during this project. The members of our research advisory committee provided us with valuable inputs. Anita Makuluni, Linda Walshire and Mary Almquist from the Public Policy Center supplied superb editorial, accounting and secretarial support.

The first author also wishes to thank his colleague, David Forkenbrock, for being a constant source of help and inspiration.

The financial support of the Minnesota Department of Transportation is gratefully acknowledged.

Executive Summary

Travel times on arterial streets provide an excellent performance measure for urban street networks. Travel time also plays an increasingly important role in advanced traffic management schemes, such as route guidance and corridor control. It is costly, however, to gather arterial travel times over an urban network, at least before the promising new vehicle detection technologies (e.g., Automatic Vehicle Identification) become cheaper and are widely implemented. It is therefore of great interest to estimate arterial travel times using data provided by existing detection technologies, such as inductive loop detectors.

This report documents our latest effort toward developing an arterial travel time model using data from conventional control/detection technologies, namely loop detectors and the Econolite ASC/2 controllers. Chapter 1 of this report briefly describes the geometric and control features of the study site, where travel time data were collected using the floating car method. Chapter 2 outlines the three-step procedure used to develop and validate arterial travel time models—data analysis, model development, and model evaluation. Chapter 3 defines a new quantity, journey speed, to replace travel time in subsequent analyses, explores the relationships between travel times, journey speeds and spot speeds, and studies journey speed patterns over various time scales: weekly, daily, and at 15-minute intervals. Chapter 4 investigates which traffic flow and traffic control parameters affect journey speed patterns most. Chapter 5 develops a number of journey speed models based on the results of Chapter 4, and Chapter 6 compares the newly developed models with two existing models. Chapter 7 summarizes major findings.

We found that average journey speed, the inverse of average travel time, is generally different from average spot speed obtained from the formula **spot speed = constant*(flow/occupancy)**. The data indicates that between these two speeds there is a strong correlation at low speeds (0–15 mph) and virtually no correlation at high speeds (>25 mph). The median and variance of journey speeds for each link are rather constant across weeks and days. For one link they vary considerably over short (15-minute) time intervals (link County Road C2–County Road C, where a lane downstream was closed during data collection.)

Among numerous traffic flow and control parameters, critical volume/capacity ratio, signal offset and the width of the green band (the latter two are closely related) have major impacts on journey speeds, and are therefore good candidate variables in travel time models. Eventually, two models are proposed:

one uses the critical volume/capacity ratio as the explanatory variable (v/c ratio model) and the other uses spot speed as the explanatory variable (spot speed model). Offset or greenband width was not used because too few observations were available in the data. The v/c ratio model yields better results in the high-speed range and the spot speed model produces satisfactory results in the low-speed range. The two models are therefore combined through a weighted average to form a third model: the combined model. After calibration, the combined model was compared with two other models, one developed by the ADVANCE project team (the Illinois model) and the other by British researchers (the British model). Results show that the combined model produces similar or better results than the other two models despite its much simpler model structure.

The limited evaluation results indicate that the proposed model is promising and can be used in the current generation of traveler information systems, where journey speeds are divided into a few ranges and each range is represented a unique color on a road network display map. For full field implementation of the proposed models, however, a number of issues need to be addressed. These issues are 1) how well the model applies to links with different geometries and controls, 2) how well it handles special events such as lane closures caused by accidents, and 3) how to extend the link journey speed model to route journey speed. We shall deal with these issues in our future research work.

Contents

List of Figures

LIST OF FIGURES

List of Tables

Chapter 1

Background

Travel time is an important parameter for evaluating the operating efficiency of traffic networks, assessing the performance of traffic management strategies, and developing real-time vehicle route guidance systems. Timely and reliable travel time data for an entire road network will be required to carry out envisioned operational tests of Advanced Traveler Information Systems (ATIS) and Advanced Traffic Management Systems (ATMS) in the Minneapolis/St. Paul area. Travel time can be obtained in a number of ways. They can be measured directly using probe vehicles or advanced detection technologies (e.g., Automatic Vehicle Identification [AVI], Automatic Vehicle Location [AVL], and video image processing), or estimated indirectly from traffic data provided by conventional detection technologies, such as inductive loop detectors. Because direct measurement of travel time is usually costly and often requires a new type of sensors, a more cost-effective method is estimation using traffic data, particularly data provided by loop detectors already in place in most signalized arterials and freeways.

There are reliable methods for estimating travel time on freeways using loop detector data. The interrupted nature of traffic flow on arterial routes, and numerous other factors that affect travel time on arterial links, however, make the estimation of travel time on arterials a much more challenging task. There have been attempts to utilize loop detector data (particularly occupancy) and signal timing parameters to estimate arterial link travel time (e.g., Gipps 1977; Gault and Taylor 1981; Young 1988; Takaba et al. 1991; Sisiopiku and Rouphail 1994). Despite the varying degrees of success achieved by these studies, few of the models developed to date have been applied to real world situations. The main reasons are two-fold: some of the models require traffic data that are not or cannot be routinely collected

from loop detectors, such as the arrival time of a vehicle at a detector and some of the models are site-specific and cannot be applied to other locations without recalibration.

In recognition of the need for an effective yet inexpensive way to estimate arterial travel time, Mn/DOT has sponsored a research project to develop a travel time estimation model using loop detector data. This project comprises of two phases. Phase I involves literature review, data collection and database development, and Phase II deals with data analysis, model development and validation. Data collected in Phase I include road geometry, travel time, detector outputs (volume and occupancy), turn volumes and signal timing. The results for Phase I has been summarized in the final report to Mn/DOT (Zhang, et. al. 1996) and won't be repeated in any detail in this report. We would, however, summarize some of the key features here for readers' benefits.

The data were collected at a site located in Roseville, Minnesota, where a 1.4 mile long route comprising of 4 links and 3 intersections was selected (Fig. 1.1) . Figs. 1.2 to 1.6 show the detailed information on road geometry and detector layout. The selected route, Snelling Avenue, is a major North-South arterial connecting metropolitan Minneapolis/St. Paul and its northern suburbs. A large trip attractor, the Rosedale Shopping Center, is also located near the study site.

Traffic at this location peaks from 7:00 am to 8:00 am for south bound traffic, and from 4:00 pm to 6:00 pm for north bound traffic. The data collection, therefore, was carried out in two periods: a morning period from 6:00 am to 9:00 am and a evening period from 3:30 pm to 6:30 pm. 10 weekdays of data in two consecutive weeks was collected and processed, producing a data base called MnLink. Tables 1.1 and 1.2 show the distances and average travel times from each intersection to the others.

Table 1.1: Link distances, in ft

Dist.	Glenhill	Lydia	Cnty Rd. C2	Cnty Rd. C	Cnty Rd. B2
Glenhill	0	2020	3270	5730	7410
Lydia	1970	0	1250	3710	5390
Cnty. Rd. C2	3220	1250	0	2460	4140
Cnty Rd. C	5620	3700	2450	0	1680
Cnty Rd. B2	7410	5440	4240	1840	0

Table 1.2: Average travel time at a prevailing speed of 45 mph, *=SB

JT (sec.)	Glenhill	Lydia	Cnty Rd. C2	Cnty Rd. C	Cnty Rd. B2
Glenhill	0	30.6*	49*	87*	112*
Lydia	30	0	19*	56*	82*
C2	48	19	0	37*	63*
C	85	56	37	0	25*
B2	112	82	64	28	0

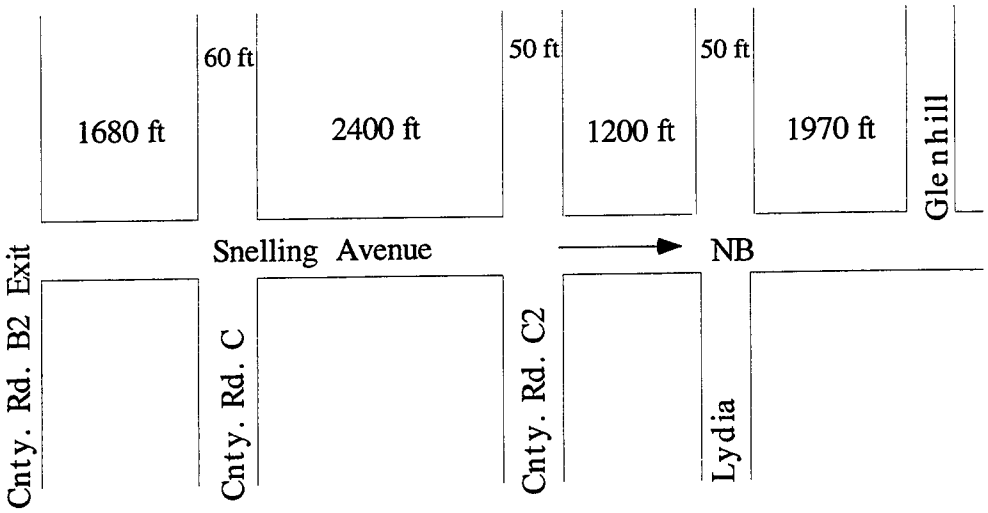

Figure 1.1: Link lengths of selected site

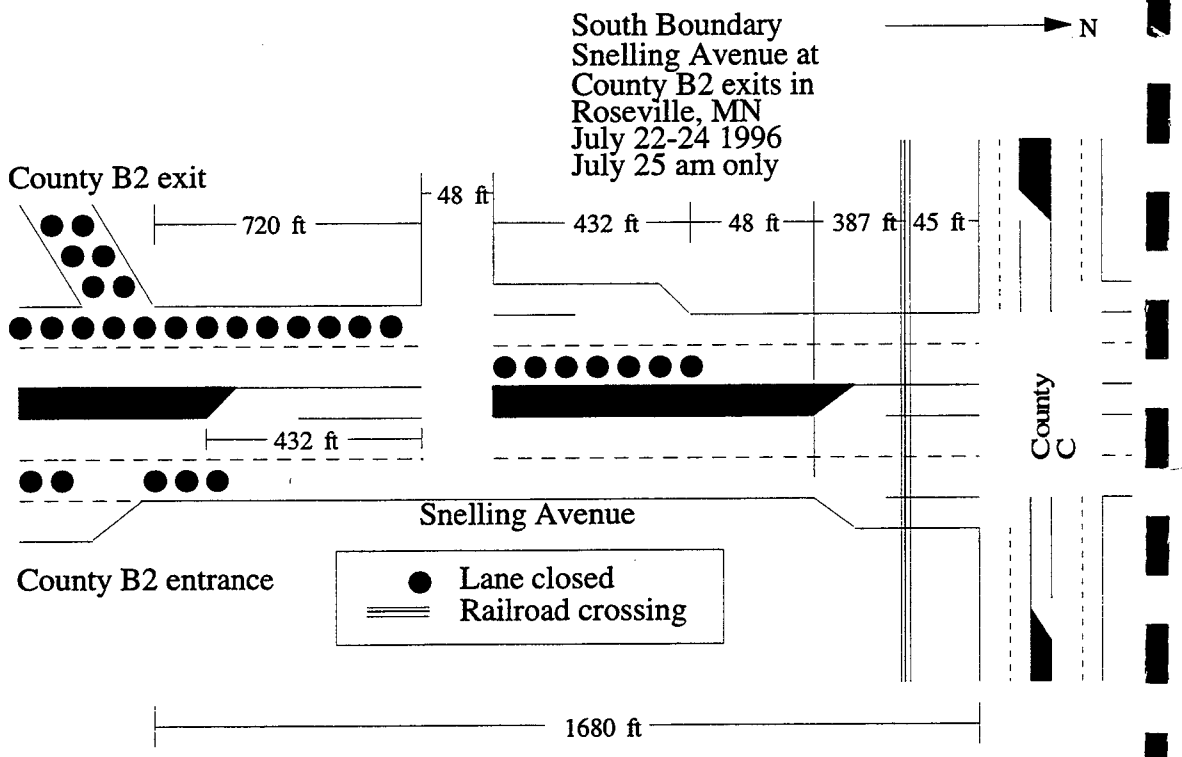

Figure 1.2: County Road B2 exit

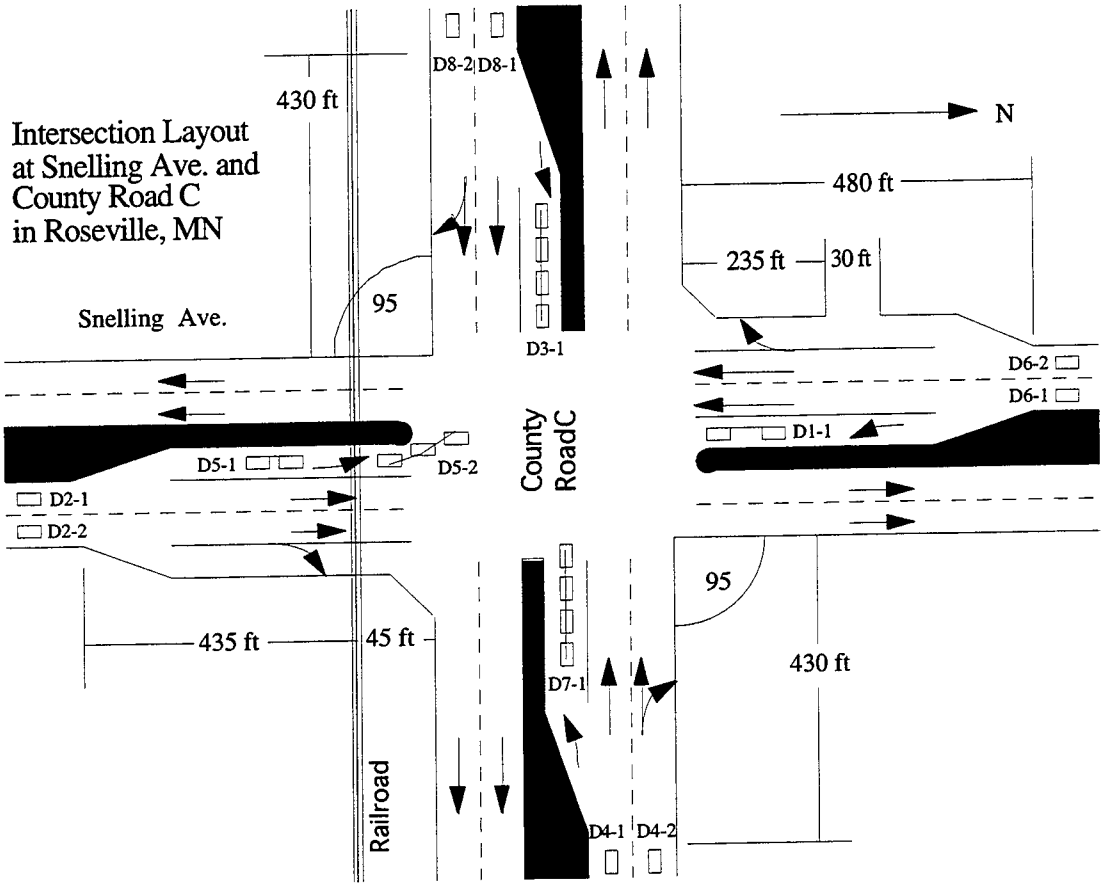

Figure 1.3: County Road C

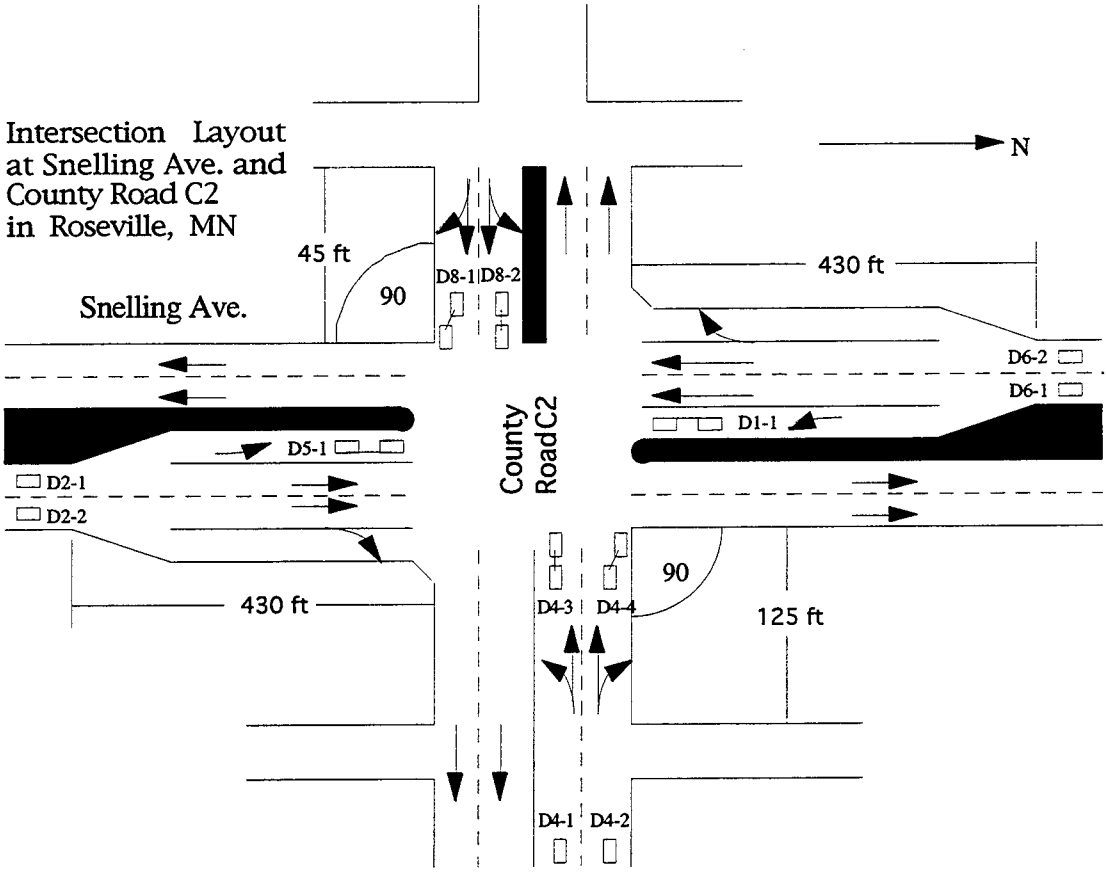

Figure 1.4: County Road C2

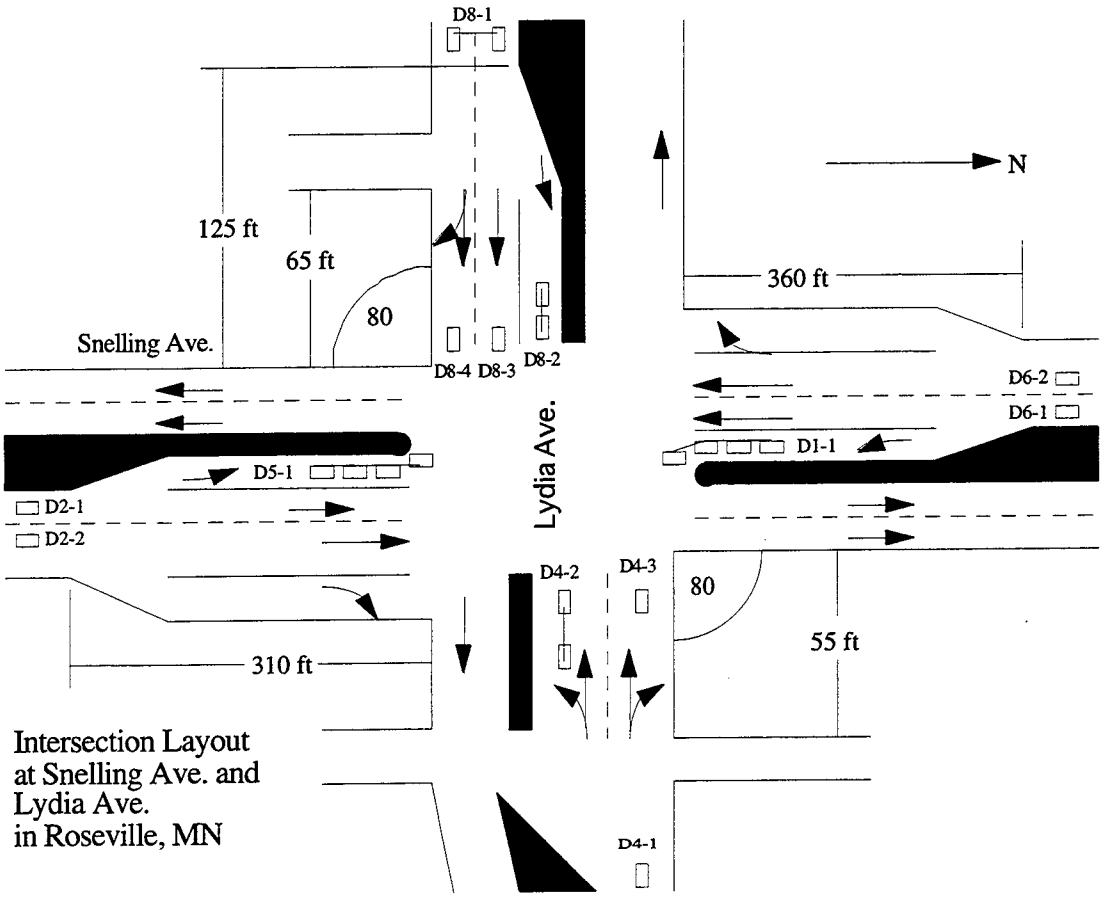

Figure 1.5: Lydia

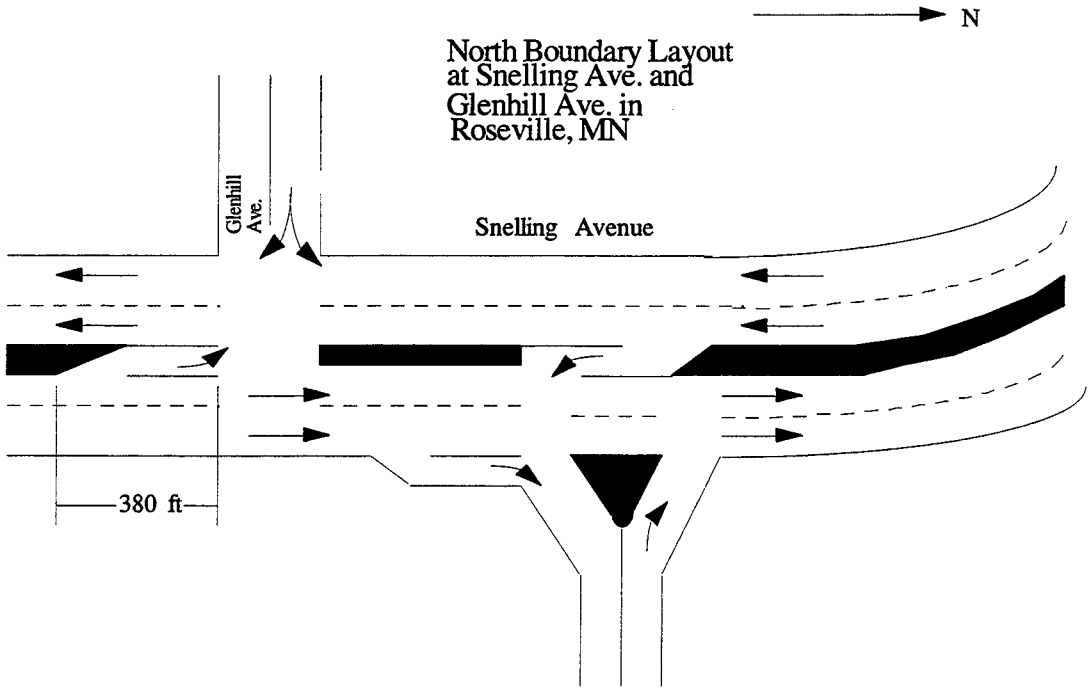

Figure 1.6: Glenhill

Chapter 2

Research Methodology

The primary objective of this project is to build an accurate, yet simple and transferable arterial travel time estimation model for Mn/DOT. Arterial link travel time is defined as the time that a vehicle takes to travel from the upstream of a link to the upstream of the successive downstream link (refer to Fig. 2.1 for definition of an link used in this study). Each arterial link usually comprises of several lanes and lane movements—through, left turn and right turn. Travel time for each of these lane movements can differ significantly. Ideally, travel time data for all the movements on a link should be collected, and models can be developed for estimating movement-specific link travel times. However, such an undertaking demands more resources for data collection and is beyond the scope of this project. As a result, only travel time for through movements was collected in the first phase. Moreover, the movement of observer vehicles during data collection was not restricted to a specific through lane, thus our travel time data are not lane specific but averages for all through lanes. The travel time models that we are going to develop are intended to estimate average link travel time for through traffic on arterial routes.

A fundamental difference between arterial and freeway travel time estimation lies in the presence of intersections on arterial streets. Travel time of a vehicle can, depending on if the vehicle is stopped by a signal, vary a great deal even when traffic are at similar demand levels. It is therefore important to consider, in addition to traffic demand, the effects of signal operations on travel time. Which signal timing parameters, or combinations of them, should be included in a travel time estimation model and what form this model should take, however, needs careful analysis.

In Phase I of this project, we have identified among various travel time

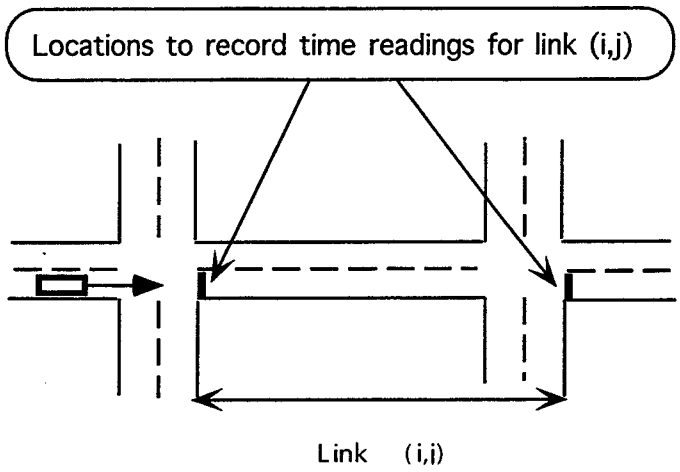

Figure 2.1: Definition of an arterial link

studies five major approaches tor arterial travel time estimation: regression, dynamic input-output, pattern matching, sandglass, and BPR. These approaches encompass a variety of travel time estimation models with diverse data requirements and application ranges. Despite the theoretical attractiveness of the pattern matching and dynamic input-output models, they have limited applicability to arterials whose traffic surveillance systems cannot provide short interval traffic data. The sandglass models, like the pattern matching and input-output models, also require traffic data (queue length) that cannot be provided by existing surveillance systems. The BPR models, on the other hand, only need volume data routinely supplied by loop detectors, but the accuracy of these models are not satisfactory for dynamic, short-term traffic management applications. Compared with the other four approaches, the regression approach is more versatile because it makes use of readily available traffic data and is capable of taking into account various factors that affect arterial travel times. It is this approach that we shall use in this project.

When regression is used in model building, there is often a danger of regressing anything against everything else. Such a practice inevitably leads to superfluous, non-transferable models. To avoid this danger, one must conduct a thoughtful analysis on the collected data to find the causal relationships among traffic variables. The insights provided by such an analysis, together with known traffic engineering principles, can then be used to guide the development of meaningful regression models. We shall refer this analysis–specification–calibration and validation model-building process as

the *system identification* approach, and explain in detail how it is realized in this project.

1. **Analyze traffic data**

   Before any travel time estimation models are developed, it would be necessary to perform a thorough analysis of the traffic data that have been collected. This analysis serves several purposes. First, it helps identify travel time patterns and reveal how these patterns differ from one location to another and from one day to another. Second, it helps identify the key traffic parameters that affect travel times. Finally, it helps ferret out the relationships among traffic variables other than travel time, which in turn can lead to simpler models.

   We would carry out this analysis in two steps. The first step studies the statistical properties of arterial travel times and looks for any travel time patterns that can be exploited in later model development. For example, if the travel time on a link has a stable pattern over days in the same time period, historical travel time data can then be used as a default in the absence of real-time estimates. It can also be combined with currently estimated travel times to improve the reliability of these estimates, or compared with current travel times to detect abnormal traffic conditions.

   The second step examines the relationships between travel time (the dependent variable) and other traffic variables (explanatory variables), as well as relationships among the explanatory variables. Link travel time typically comprises running time and stopped delay at a signal. Running time is largely dependent on average flow speed, link length, and traffic composition. In the absence of special events such as accidents or adverse weather conditions, running time is expected to be fairly stable and predictable. The variations in travel time therefore come mainly from stopped delays, which are much harder to predict. Factors that influence stopped delays are numerous—traffic demand level, traffic composition, turn movements, signal timing, intersection layout, and so forth. For example, good signal progression could make platoon of vehicles travel through a couple of intersections without stops, which leads to no or little signal delays and therefore shorter link travel times. As a result, one would expect that link travel time would be somewhat related to signal offset, a parameter that determines the level of progression. By performing statistical analyses on the data, we would be able to find out how these factors and/or their

combinations influence travel time.

Although the factors that affect arterial travel time are numerous, many of these factors are not completely independent of each other. For example, volume and occupancy are strongly correlated. The green splits of a signal cycle in a traffic-responsive control plan are also related to the demand level at various approaches. Finding such relationships can help reduce the number of variables in a model and avoid multicollinearity in model specification. It also helps develop estimators of those variables that are not directly available from field data but play important roles in determining arterial travel times.

2. **Develop improved travel time models**

   The data that we have collected allow a richer model specification than many of the previous studies can do. The data include turn counts (left and right turns), signal plans, stopped delays at intersections, occupancy and volume in shorter time intervals (five minutes). All this information could be utilized to develop a more accurate travel time model. The accuracy of a model may be increased by considering as many factors as one can. This, however, would certainly make the resulting model more complex and harder to calibrate, and might obscure the effects of each independent variable on travel time. Because the explanatory factors are not completely independent of each other, we can exploit their inter-relationships to reduce significantly the number of variables in the model, while retaining its accuracy. For example, the intersections where our data were collected are under traffic-responsive signal control. This control calculates a traffic flow index CLEV (Computed LEVel) based on a combination of factors (e.g., volume and occupancy), and generates a timing plan according to this index. As such we would expect that the green splits in a signal cycle are closely related to the demand and occupancy levels of various approaches. Rather than putting all the variables including volume, occupancy, and green splits into a regression model, we may use volume/saturation flow rate (degree of saturation) and cycle length to replace the green splits, such that the model has less variables but retains the same explanatory power as the model that includes green splits. Or we might even find that the CLEV index is as good an explanatory factor for travel time as volume and occupancy combined. In that case, we would obtain a much simpler model of travel time based on the CLEV index.

Of particular interest to traffic management centers is the accurate estimation of travel time under abnormal traffic conditions, because it is precisely at such times that travel time information is more useful to travelers. These abnormal traffic conditions can be caused by traffic accidents, signal failures, or other special events, all of which are hereafter referred to as incidents. To accurately estimate travel time under incident conditions, one has to consider carefully the traffic patterns generated by these incidents. For example, a mid-block lane-blocking accident may cause congestion at the upstream intersection but not at the downstream one. Because of this fact, a link travel time model that uses only traffic data from the downstream intersection on a link may not be able to produce reliable travel time estimates when the link has a mid-block lane-blocking accident. Under such a situation, a model that uses detector data at both intersections would have a better chance of capturing the impact of a mid-block accident on travel time. We would explore various model specifications capable of capturing the effects of incidents on travel time. The resulting model, if successfully developed, would in turn aid the future development of arterial incident detection algorithms based on travel time.

Model building certainly involves experimentation. Based on the insights provided by analyses of the data and previous studies reviewed in Phase I of this project, various model specifications will be explored. Careful attention would be given to model accuracy, simplicity, and transferability. Other factors, such as availability of data in field operations, would also be considered during the model-building process.

3. **Validate the developed models**

The developed models will undergo limited laboratory evaluation before they are tested in field operations. The planned laboratory testing comprises two steps. The first step evaluates the models' performance using data collected at the same site but on different days. The second step, depending on the availability of data, tests the models' accuracy and transferability to other sites. A number of existing travel time models will also be calibrated using the MnLink data set and their predictions be compared with the newly developed models.

Through model validation and comparison, we hope to find the weaknesses of the newly developed models and continue to address those weaknesses and improve the models as our research progresses.

Chapter 3

Travel time/journey speed patterns

3.1 Journey speed versus spot speed

Before proceeding with our analysis, we first define a new quantity, journey speed, to replace travel time. The journey speed u_j of a link j is simply the length of the link divided by the time required to traverse that link. In our subsequent analysis, we use the journey speed rather than travel time of a link to indicate the level of congestion on that link. This substitution has several advantages:

1. it allows comparison of congestion levels between links of different lengths,

2. it is intuitive to travelers and consistent with the congestion indicators used on the freeway network, therefore are applicable to integrated traffic management systems,

3. it possesses nicer statistical properties for analysis[1].

It should be noted that journey speed is different than the travel speed measured by paired loop detectors, which we refer hereafter as spot speed.

[1]The travel times are not normally or Gaussian distributed. After a Box-Cox transformation, the transformed data are normally distributed. Therefore we can make inference with predetermined confidence regarding some useful properties of the data. This transformation turns out to be the inverse of the travel time, which has a natural interpretation as average travel speed.

Journey speeds take travel delays at intersections into account, and are usually smaller than speeds measured by loop detectors (this will be discussed further in sections below).

Because spot speeds are often more readily computable than journey speeds, it is often an enticing idea to substitute journey speed with spot speed for arterial traffic, as one usually does for freeway traffic. This approach, however, generally does not work. Although there is a relationship between spot speeds and journey speeds under certain traffic conditions, great care needs to be taken to substitute one speed with another.

Before presenting the results obtained from analyzing the MnLink data, we first show the procedures for estimating spot speeds from volume and occupancy information measured by inductive loop detectors.

We know that the occupancy measured by a detector, o is proportional to the local density ρ

$$o = 100\overline{L}\rho \tag{3.1}$$

where $\overline{L}$ is the average effective vehicle length of the traffic stream that passed the detector during the sampling interval T. This length comprises two parts: vehicle length and the length of the loop detector. Assuming an average of 14 ft for a vehicle and 6 ft for a loop detector, we have $\overline{L} = 20ft$. This would yield

$$o = 0.379\rho \tag{3.2}$$

From traffic flow theory, we also know that flow rate q, density ρ and local space mean speed u observes the following relationship

$$q = u\rho \tag{3.3}$$

Based on Eqs. 3.2 and 3.3 we can calculate the local speed for a single lane as

$$u = 0.379\frac{q}{o} \tag{3.4}$$

For multilane traffic, we average the speeds obtained using Eq. 3.4

$$\overline{u} = \frac{1}{N}\sum_{i=1}^{i=N} u_i \tag{3.5}$$

where N is the number of lanes in an approach for which travel time is measured.

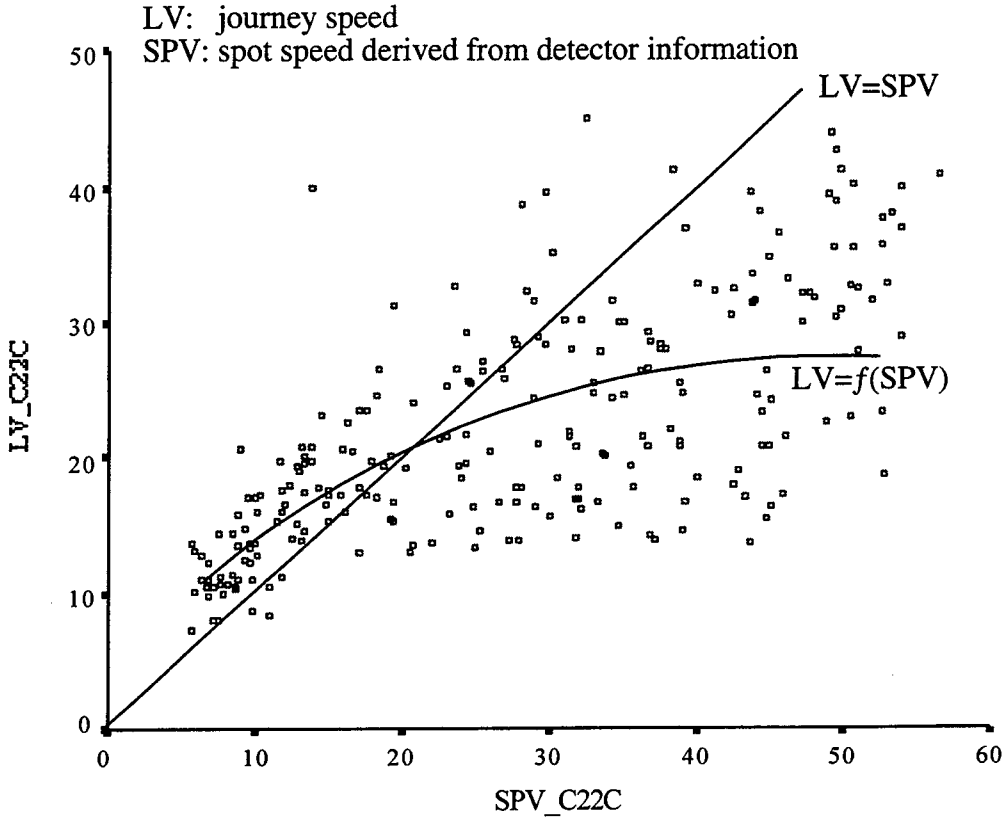

Figure 3.1: Journey speed vs. spot speed, SB C2 to C link

It is clear from Fig. 3.1 that spot speeds overestimate journey speeds when there is no congestion, and the relationship between them are rather weak (Fig. 3.2). This is not surprising because spot speed measures average speed at a fixed point, where faster traffic tends to be over-represented than slower traffic. On the other hand, journey speed measures the average speed over a length of road way, where both slow and fast portions of the journey are duely represented. It should be noted that at lower speed range, however, spot speeds underestimate journey speeds. This is because for congested traffic, queues in front of a signal leads to fairly low spot speeds that do not take into account the travel speed during the unstopped portion of the journey.

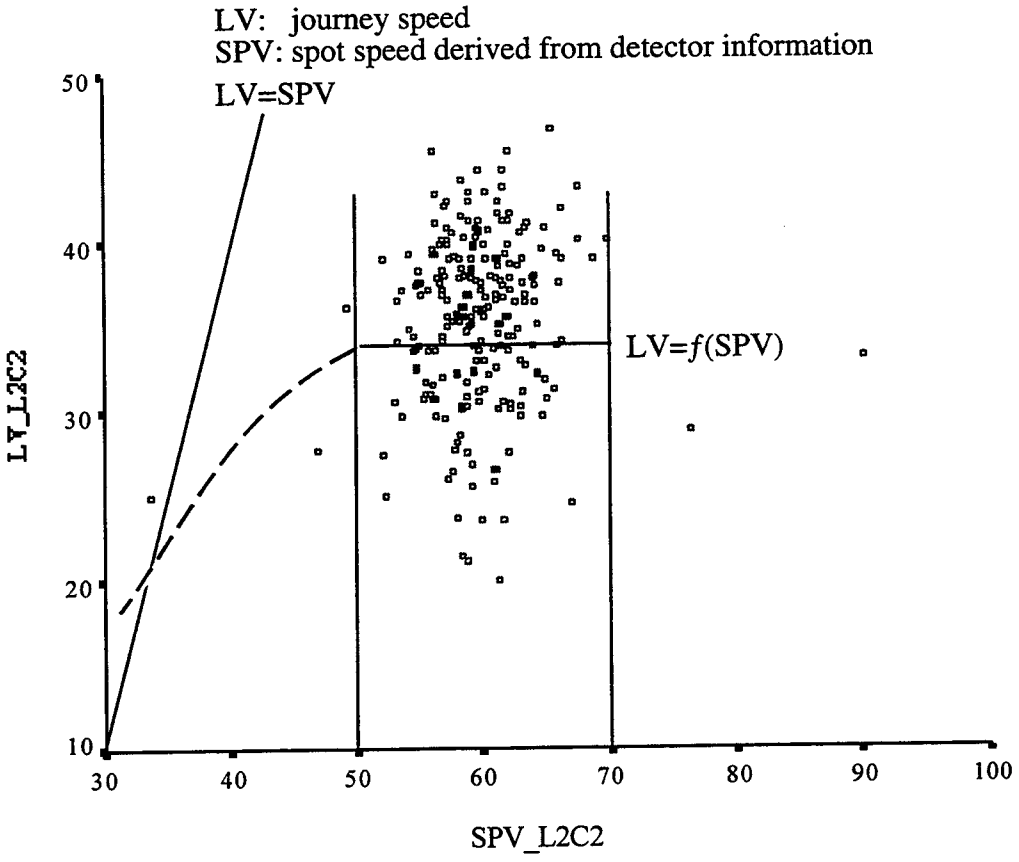

Figure 3.2: Journey speed vs. spot speed, SB Lydia to C2 link

Spot speed is nonetheless very useful information for predicting congestion on arterial links, and should be fully utilized. Rather than direct substitution of journey speed with spot speed, one can develop the nonlinear relationship, as evident in Fig. 3.1, to estimate journey speed from spot speed. This would, based on the analysis of MnLink data, produce reliable estimate of journey speed for congested traffic. It does not, however, give good estimates of journey speeds for uncongested traffic (see Fig. 3.2). Because it is prcisely the congestion information that we are seeking, the latter does not appear to be a severe limitation for practical applications.

3.2 Journey speed patterns

Traffic in urban areas often has distinctive patterns. For example, there are usually two peak periods, the morning and the evening peak, when traffic demand is high. In fact, these patterns are more or less rather stable over time for many locations unless significant shifts in demand or special events occur. Stable traffic patterns over time yield higher predictability for travel time and would be first examined in this analysis.

We study journey speed patterns using a tool called *boxplot*, a plot based on *quartiles*[2], *median* and *extreme values*. A boxplot contains a box (consisting the 25% and 75% quartile), the median (a thick line within the box), whiskers (the minimum and maximum values excluding extreme values) and extreme values. Extreme values include *outliers* (values within 1.5-3 box-length from upper or lower edge of the box), and extreme values (values more than 3 box-length away from the upper or lower edge of the box). Apart from these information, a box-plot also conveys information about spread and skewness.

The following sections present the results obtained from analyzing journey speeds on route Glenhill – C2 and links Lydia – C2 and C2 – C for south bound traffic. The analysis was carried out separately for morning and evening traffic because of our prior belief that these two periods would have different traffic patterns.

3.2.1 Weekly patterns

Figs. 3.3 and 3.4 show the average journey speeds in weeks 1 and 2 for route Glenhill to County Road C. While the median journey speeds in the morning are generally higher than those in the evening, they are not much

[2]Quartiles are values that divide a sample into four equal-sized groups

different across weeks in either morning or evening. It is noted that morning journey speeds appear to have larger variations than evening journey speeds (normal plots indicate that morning journey speed is normally distributed, while evening journey speeds is nearly normally distributed).

Similar conclusions can be drawn for link journey speeds on links Lydia to C2 and C2 to C (Figures 3.5 to 3.8). Some differences, however, exist. Median journey speeds in morning and evening periods for link Lydia to C2 are nearly identical. But for link C2 to C, morning median journey speeds are higher than evening median journey speeds. Furthermore, the journey speeds on C2–C link have large variances and skewed distributions in both the morning and evening periods.

These figures clearly show that the daily averages of journey speeds on the chosen site are stable over weeks. Next we examine if average journey speeds change significantly across weekdays.

3.2.2 Daily patterns

The daily average journey speeds for links Lydia to C2 and C2 to C are shown in Figures 3.9 to 3.12. These patterns have strong resemblance to the weekly patterns: for each period (morning or evening), a link's daily average journey speeds are not much different across days. They differ between periods for some links (link C2 to C) and show very little difference for other links (link Lydia to C2).

3.2.3 Short interval patterns

We have studied patterns of long time averages (weekly and daily) of route (link) journey speeds, and found that these averages are stable across weeks and weekdays. We now examine the journey speed patterns in shorter time intervals. To ensure a representative short time average, we use 15 minute time intervals in our analysis. Figures 3.13 to 3.16 show the boxplots of journey speeds on links Lydia to C2 and C2 to C in 15-minute intervals for both morning and evening traffic. The median journey speeds for link Lydia to C2 are rather constant in both morning and evening periods. Those for link C2 to C, however, are drastically different between morning and evening, and between different times of day. There is a clear peak period in the morning when journey speeds are significantly lower than other periods. The evening median journey speeds for this link are rather low and constant, but variations of evening journey speeds are fairly different across periods:

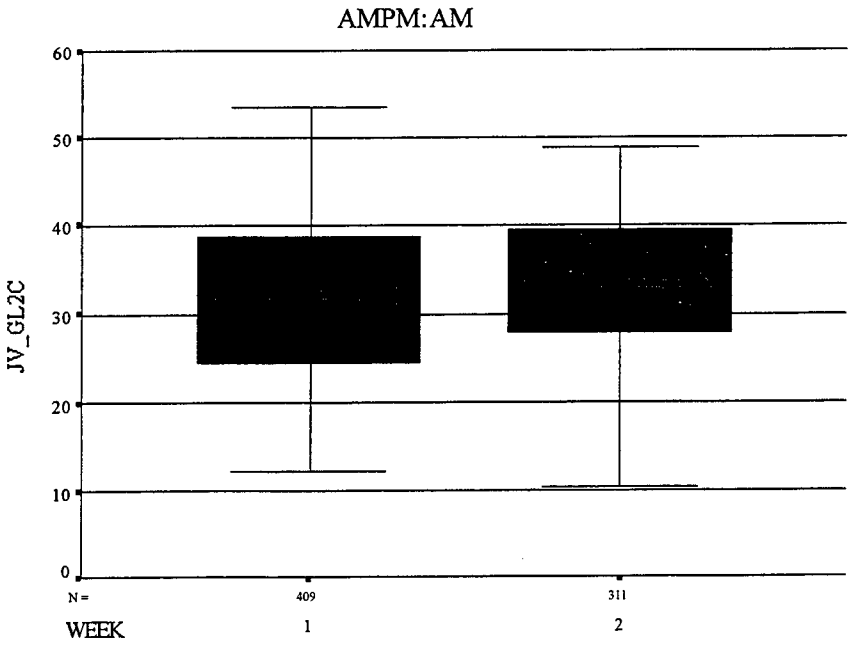

Figure 3.3: Weekly pattern, AM route journey speed, Glenhill to C

the scatter is much narrower in the peak period than the non-peak periods[3].

The wide scatter of journey speeds at some periods can be attributed to the fewer number of travel time observations made in those time periods. Depending on if the observing vehicle stopped at the link intersection, journey speeds can vary significantly in light traffic conditions. The few observations made under such conditions therefore could differ a great deal, resulting in large variations in journey speeds. When traffic is congested, on the other hand, the observing vehicles following the flow are more representative of stream travel times, thus leads to smaller variations in journey speeds.

The box plots have shown distinctive journey speed patterns in short time intervals. If these patterns could be related with appropriate traffic flow and signal timing patterns, models can be developed to predict journey speeds, therefore travel times using those traffic parameters. We will examine in the following sections, that how much of the journey speed patterns are explainable by traffic flow patterns and signal timing parameters.

[3]Perhaps the variance to mean ratio is a better measure of scatter than just variance.

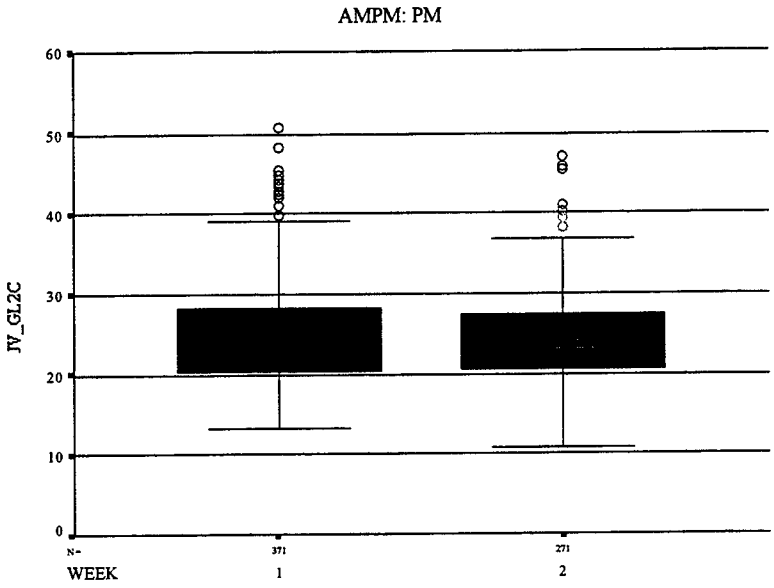

Figure 3.4: Weekly pattern, PM route journey speed, Glenhill to C

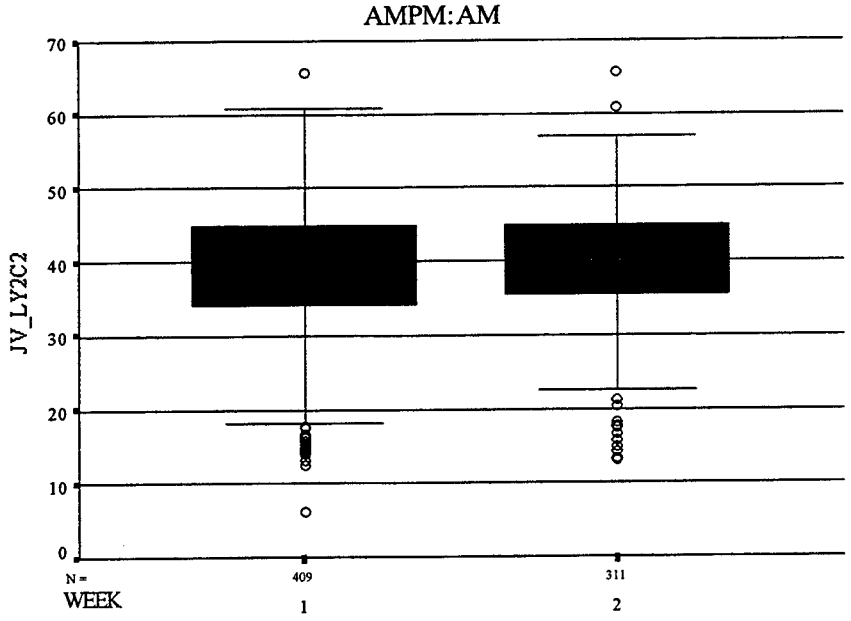

Figure 3.5: Weekly pattern, AM link journey speed, Lydia to C2

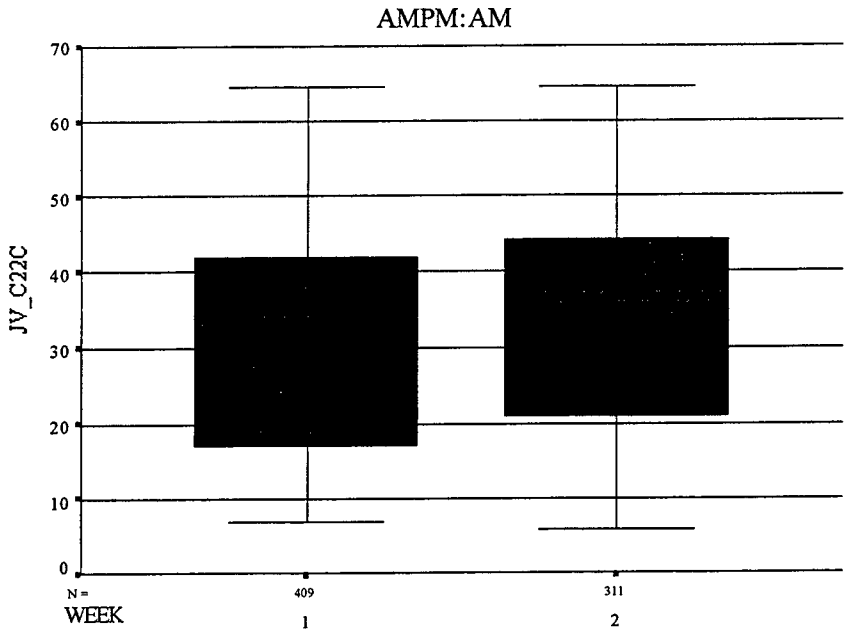

Figure 3.6: Weekly pattern, AM link journey speed, C2 to C

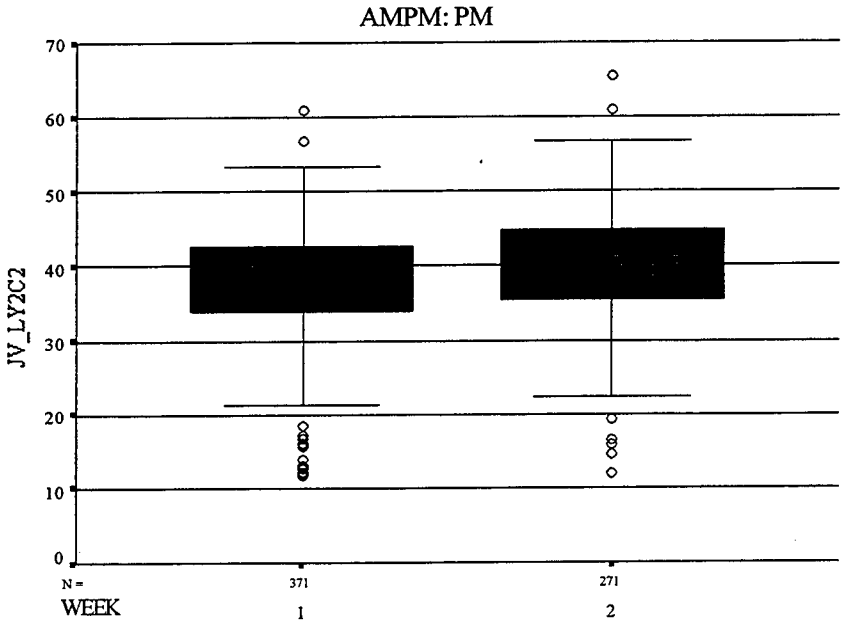

Figure 3.7: Weekly pattern, PM link journey speed, Lydia to C2

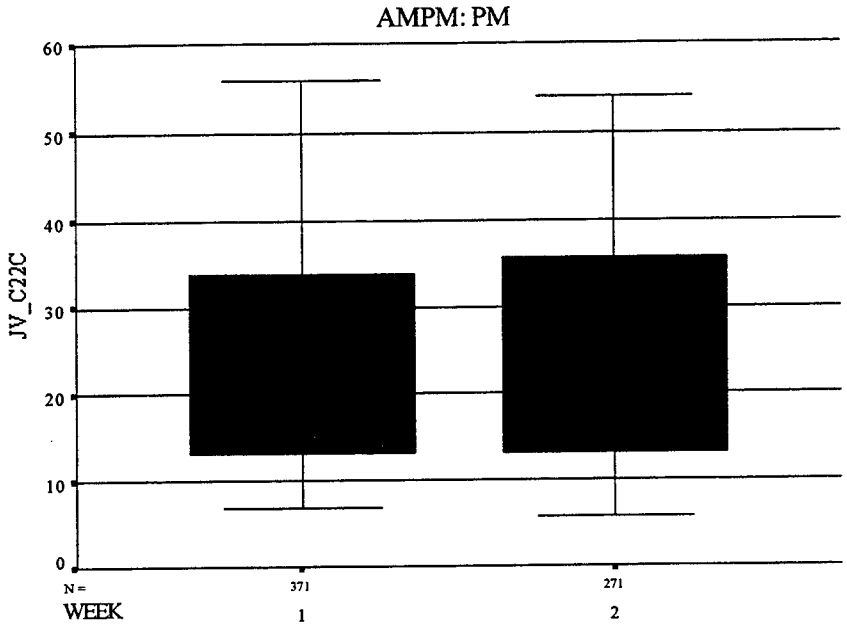

Figure 3.8: Weekly pattern, PM link journey speed, C2 to C

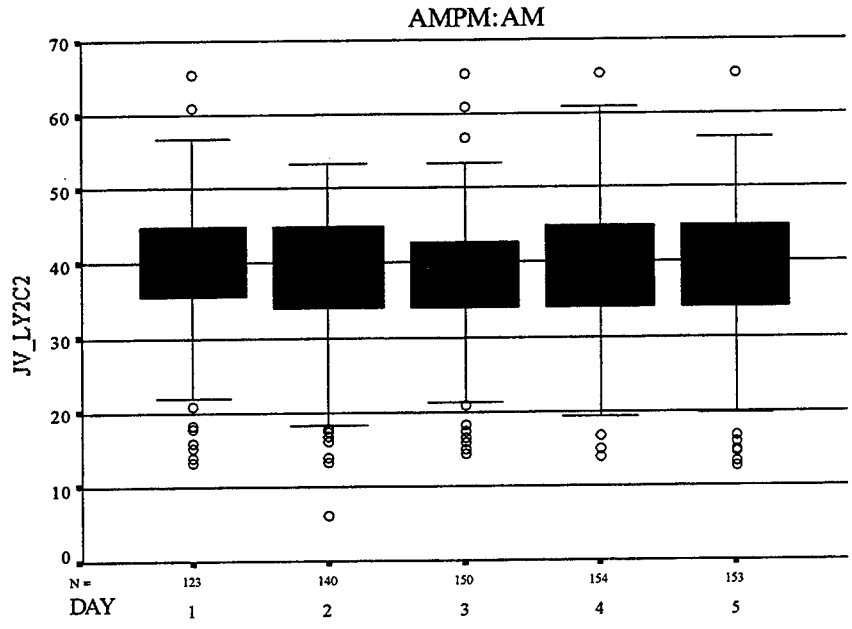

Figure 3.9: Daily pattern, AM link journey speed, Lydia to C2

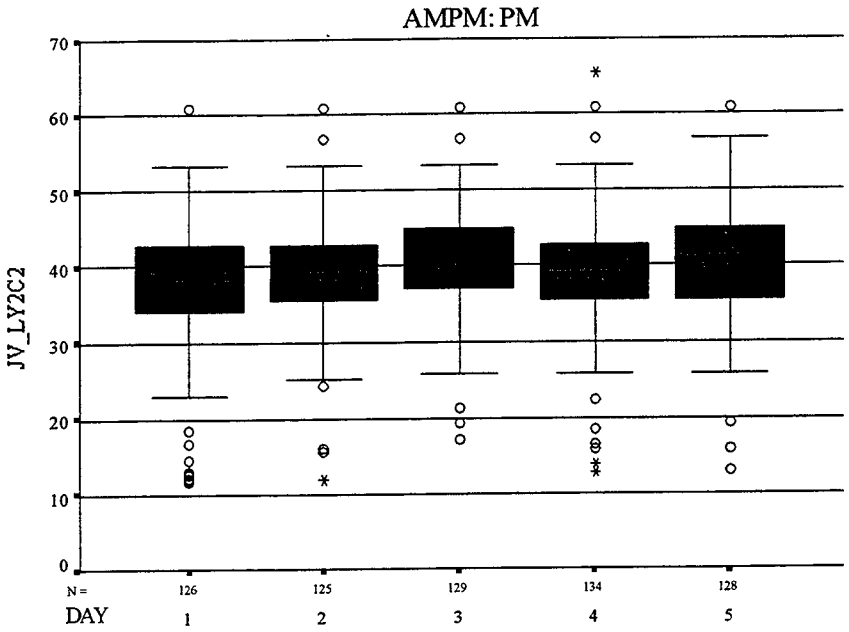

Figure 3.10: Daily pattern, PM link journey speed, Lydia to C2

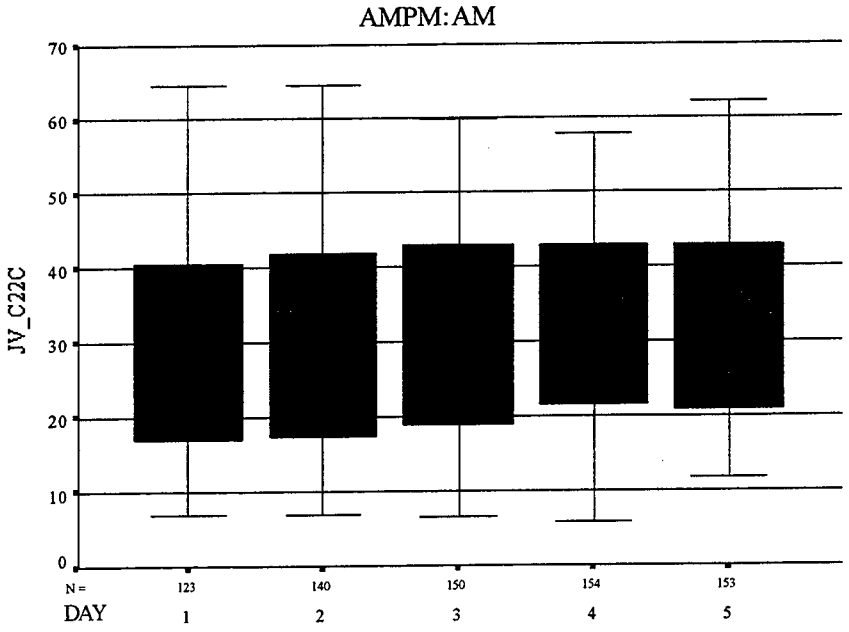

Figure 3.11: Daily pattern, AM link journey speed, C2 to C

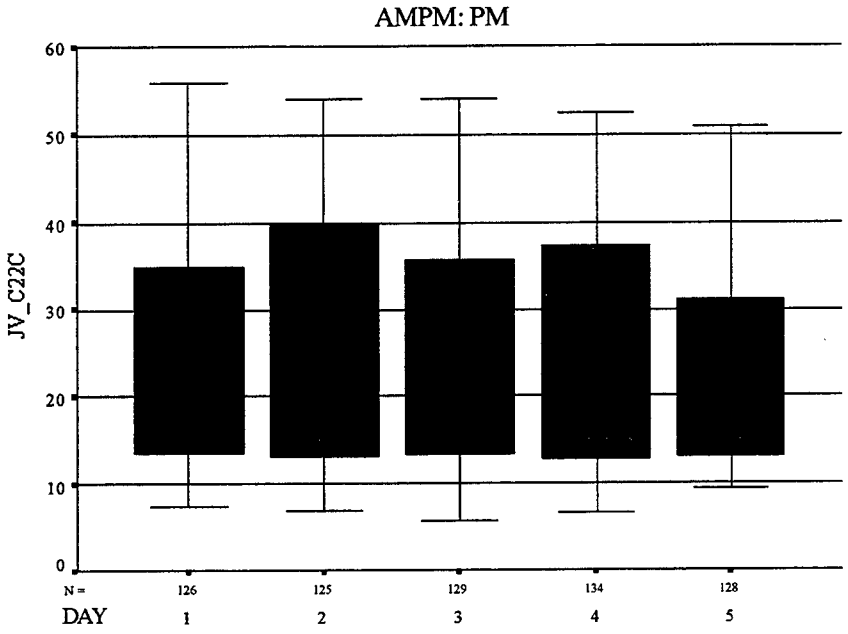

Figure 3.12: Daily pattern, PM link journey speed, C2 to C

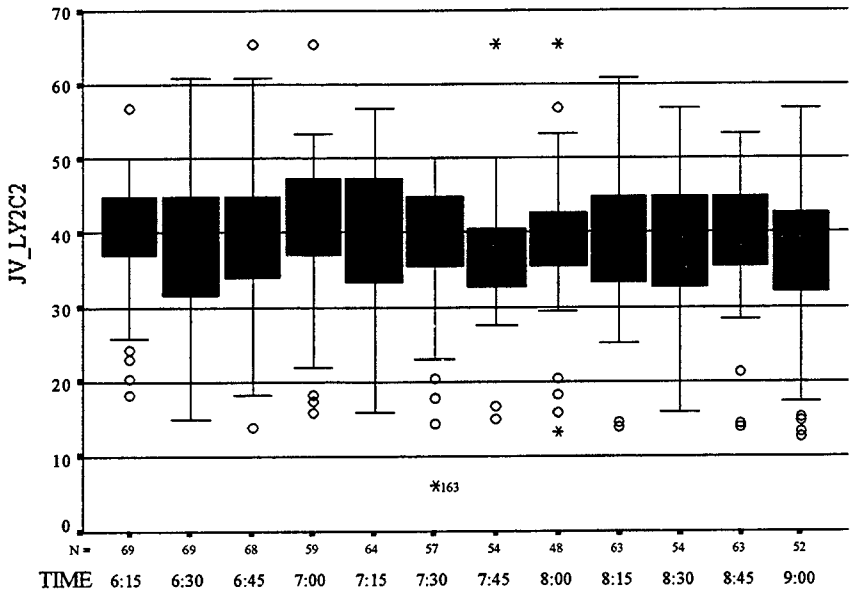

Figure 3.13: Short interval pattern, AM link journey speed, Lydia to C2

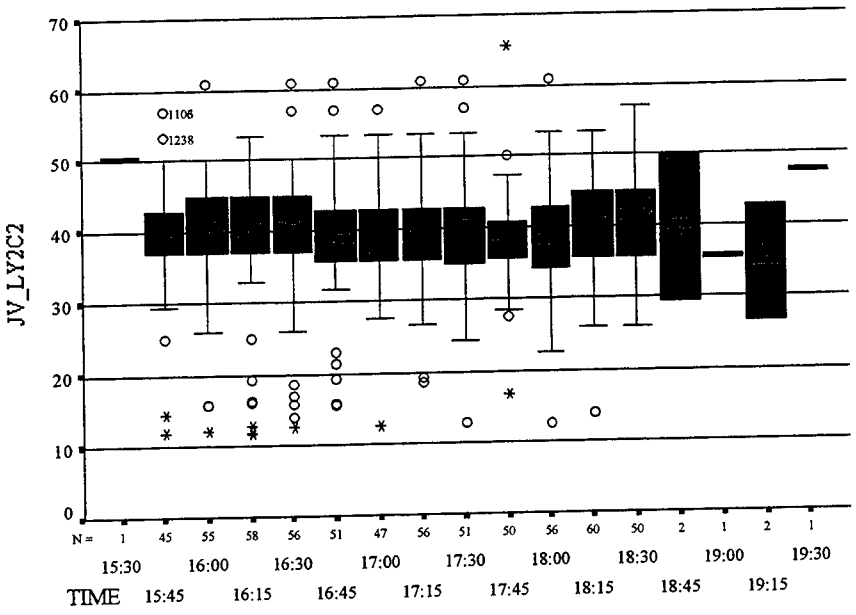

Figure 3.14: Short interval pattern, PM link journey speed, Lydia to C2

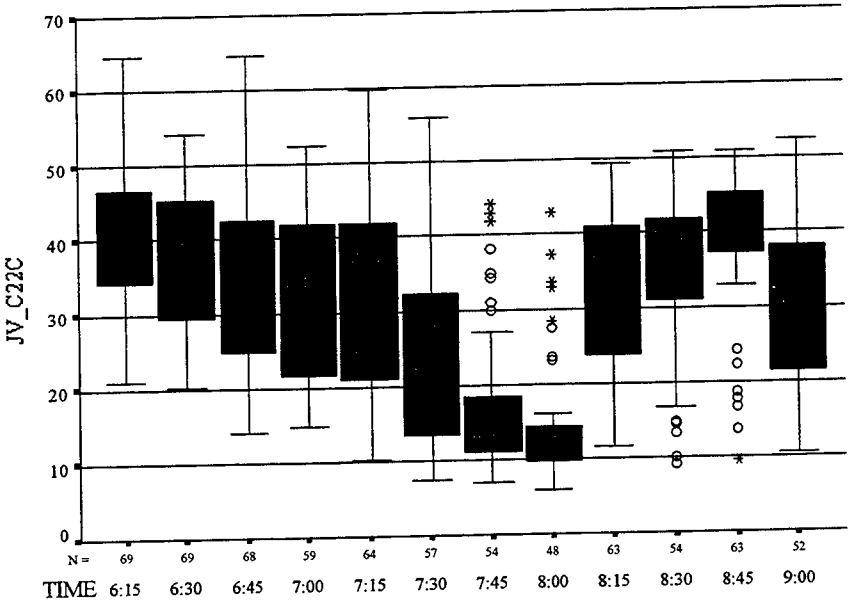

Figure 3.15: Short interval pattern, AM link journey speed, C2 to C

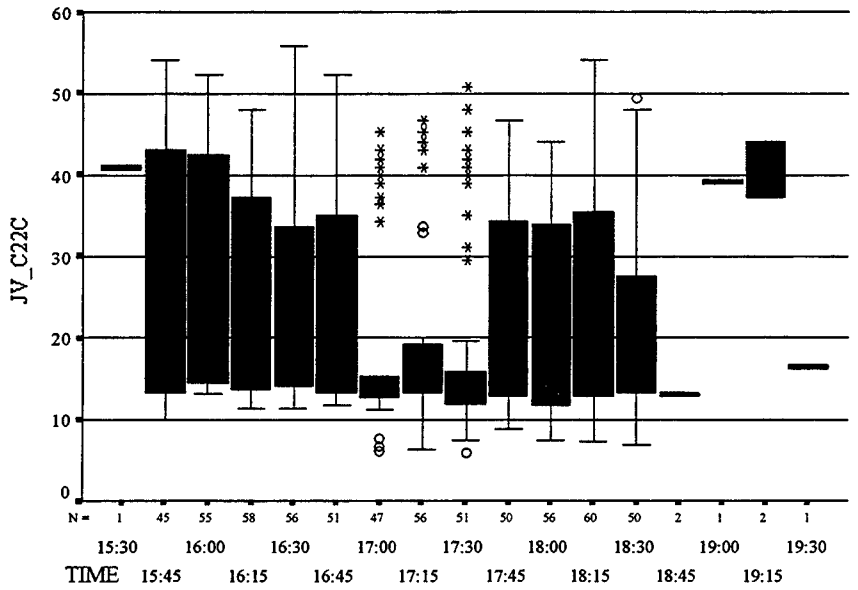

Figure 3.16: Short interval pattern, PM link journey speed, C2 to C

Chapter 4

Factors that affect journey speeds

We have seen in Section 3.2 that journey speeds for arterial links have distinctive patterns over time (in 15 minute intervals). This chapter attempts to anwser the question that how much, if any, these patterns are related to traffic demand patterns and intersection signal settings. For brevity, we will skip the detailed statistical analysis procedures and present only the results. Since our ultimate goal of this research is to build a travel time estimation model for short term travel time prediction, we limit our analysis to the demand patterns over a short time interval (15-minute).

4.1 Traffic flow patterns

This section studies the effects of three parameters on journey speeds. These three parameters are total demand, maximum lane occupancy and traffic distribution across lanes. The total demand is obtained by adding all the demands for the two through lanes, maximum lane occupancy is the larger occupancy of the two through lanes, and traffic distribution is described by a ratio between the minimum through lane traffic flow and the total through lane flow.

Because link Lydia to C2 is the immdediate upstream link of link C2 to C, we would expect that the demand and occupancy patterns for both links are similar if traffic could travel without being interrupted by the two intersections at C2 and C. In the morning period, the demand patterns for both links are indeed resemblant: both have a distinctive peak period around 8:00 am with similar peak flows (Figs. 4.1 and 4.2). The corresponding

journey speeds for both links during this period, however, are strikingly different (Figs. 3.13 and 3.15). Journey speeds on link Lydia to C2 is much higher during this peak period than those on link C2 to C in the same time period. In fact, journey speeds on link Lydia to C2 are marginally different than those in non-peak periods despite that the demands are much higher in the peak period than in the non-peak periods. The variation in journey speeds, therefore, cannot be fully explained by demand patterns alone. If we look at the maximum lane occupancy for both links, we would find that the occupancy level for link C2 to C is rather high (in the range of 30 to 60) during the peak period, while the occupancy level for link Lydia to C2 is fairly low (below 10) during the whole morning period (Figs. 4.3 and 4.4).

Why does there exist such large differences between journey speeds of two links with similar demand? The answer lies partially in how traffic is serviced at the two link intersections, intersection C2 for Lydia to C2 and intersection C for C2 to C. To support this argument, we calculate the traffic distribution across lanes by dividing the lowest lane volume with the total lane volume for the two through lanes at both intersections. Figs. 4.5 and 4.6 show the lane distributions of traffic flow during the morning peak for the two through lanes. The distribution for C2 to C link is fairly unbalanced, with one lane sharing about 80 to 90 percent of the total demand; while that for link Lydia to C2 is much more balanced, with a 40 to 60 percent share among lanes[1]. Because one lane at C is not fully utlized, the demand for intersection at C exceeds its operating capacity, leading to long delays and lower journey speeds.

Although the evening traffic patterns are not as distinctive as the morning patterns (the peaks are more spread), they tell roughly a similar story: demand levels at both links are similar, but occupancy and lane distributions are quite different for the two links, with link C2 to C having high occupancy levels and low journey speeds throughout most of the time periods (Figs. 4.7 to 4.12).

4.2 The influence of signal offsets

It is clear from Section 4.1 that traffic demand patterns cannot fully explain the journey speed variations for certain links. This is not surprising because,

[1]It is known to us that a lane closure 500 ft downstream of intersection C caused the unbalanced traffic distribution across lanes. For automatic incident detection or journey speed estimation, however, such information is not available apriori and parameters such as lane traffic distribution could be used to infer about occurances of incidents or lane closures.

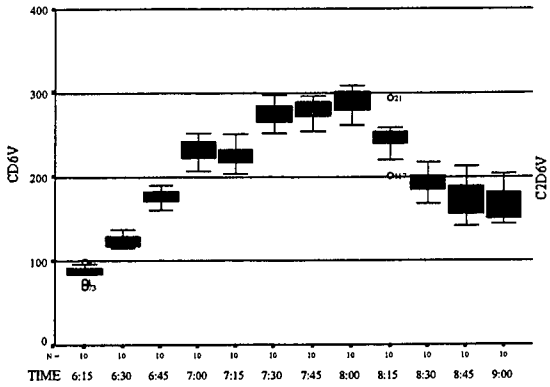

Figure 4.1: Demand pattern at C, SB morning traffic

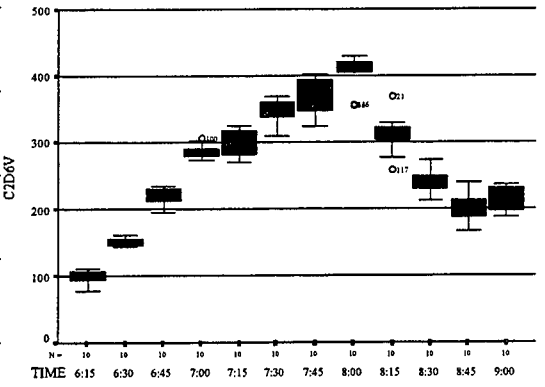

Figure 4.2: Demand pattern at C2, SB morning traffic

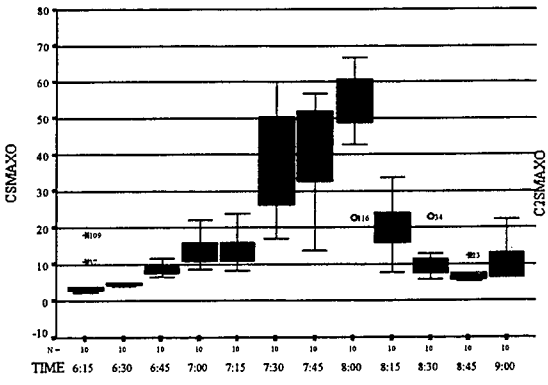

Figure 4.3: Occupancy pattern at C, SB morning traffic

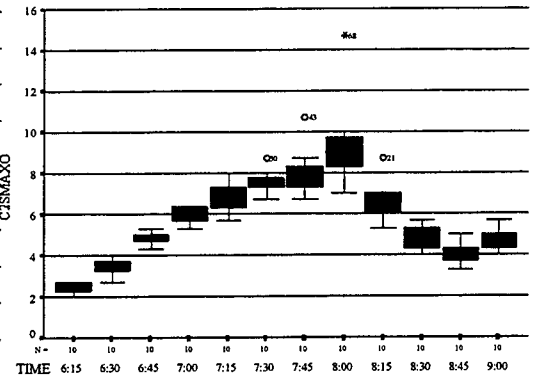

Figure 4.4: Occupancy pattern at C2, SB morning traffic

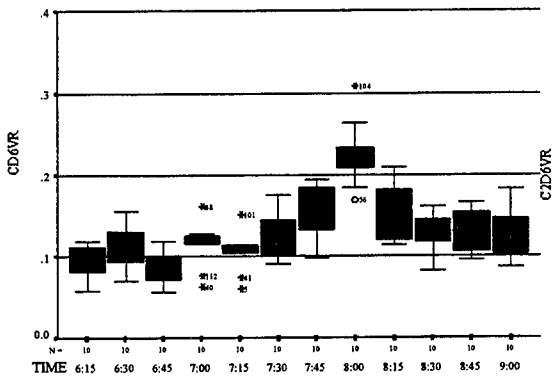

Figure 4.5: Traffic distribution across lanes, SB morning traffic at C

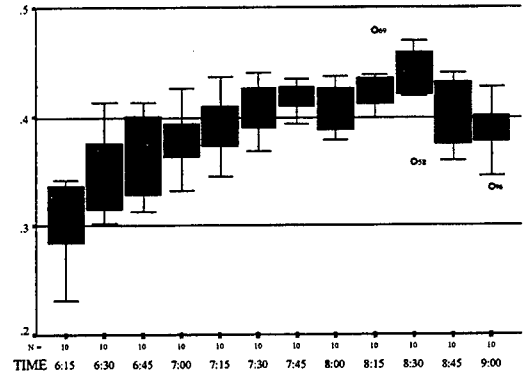

Figure 4.6: Traffic distribution across lanes, SB morning traffic at C2

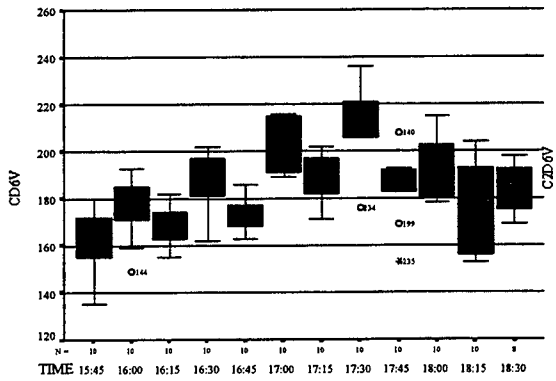

Figure 4.7: Demand pattern at C, SB evening traffic

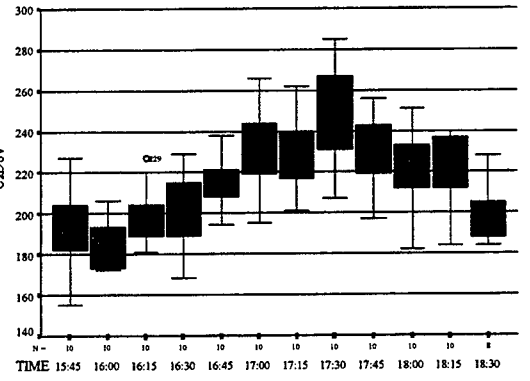

Figure 4.8: Demand pattern at C2, SB evening traffic

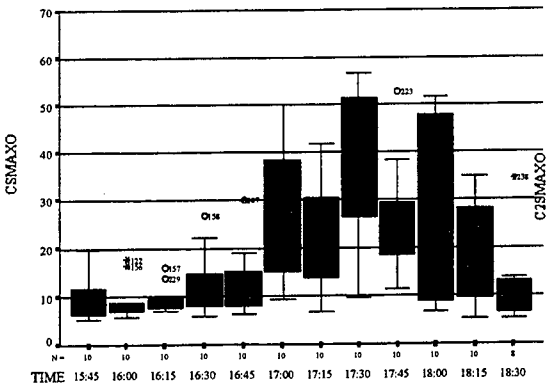

Figure 4.9: Occupancy pattern at C, SB evening traffic

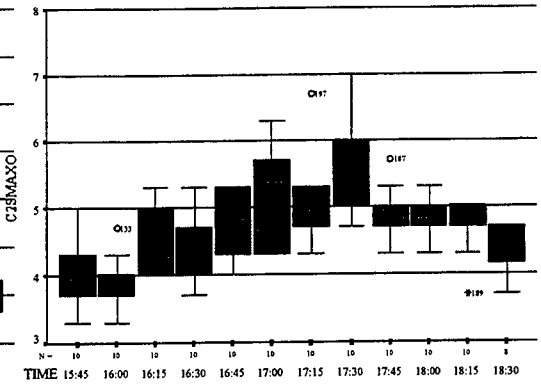

Figure 4.10: Occupancy pattern at C2, SB evening traffic

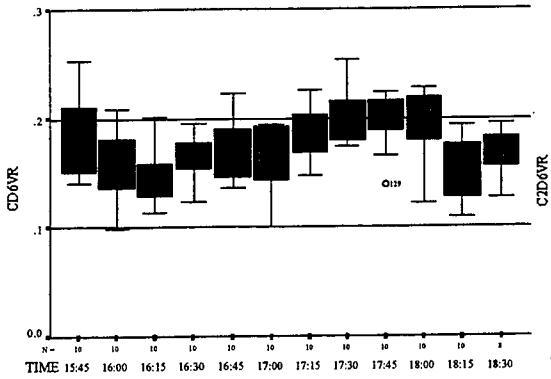

Figure 4.11: Traffic distribution across lanes, SB evening traffic at C

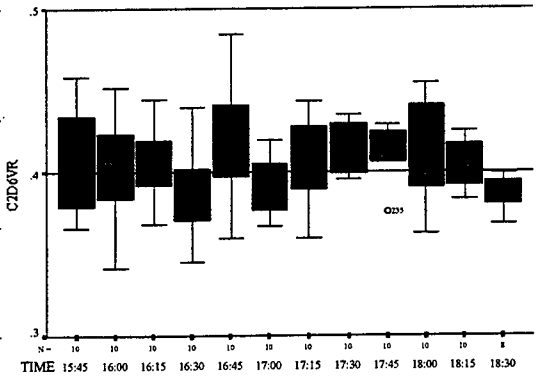

Figure 4.12: Traffic distribution across lanes, SB evening traffic at C2

as we discussed in Chapter 2, that the periodic interruption of traffic flow by intersection signals is a key factor affecting arterial travel times, therefore journey speeds. This section studies the effects of one signal parameter, offset, on journey speeds.

Signal offset is a parameter that controls the initiation or ending of green of a particular phase in a signal timing sequence such that a platoon of vehicles can travel through a series of intersections without stopping. Well coordinated signals can provide good progression for traffic in the designated offset direction and usually lead to fewer number of stops and higher journey speeds.

The three intersections at the study site are controlled by a master controller and three local controllers operating under traffic responsive mode. In this mode, the controllers gather volume and occupancy information from system detectors and calculate four paramters: CLEV (computed level) , COFT (computed offset), SPL/SF (split/special function) and ART/NRT (arterial/non-arterial). These parameters are then used to determine the cycle level (CYC, 1–6), offset (OFT, 1–3) and split (SPL, 1–4) (C.O.S.) combinations that map traffic conditions with one of 64 predetermined signal timing plans.

The following analysis uses data from July 15, 1997. There are six traffic signal plan changes during the morning period on this day, which is shown in Table 4.1, and three signal plan changes in the evening period, which is shown in Table 4.2.

Table 4.1: Signal plan changes, morning traffic, 7/15/96

trans. time	CLEV	COFT	SPL/SF	ART/NRT	c.o.s	cycle (s)	offset
6:14 am	2	A	1	ART	6.1.1	75	1
6:36 am	3	A	1	ART	30	–	–
6:38 am	3	1	1	ART	3.2.2	120	2
7:22 am	4	1	1	ART	4.2.2	134	2
8:46 am	3	1	1	ART	3.2.2	120	2
8:48 am	3	A	1	ART	30	–	–

There are four C.O.S and ART/NRT combinations in the morning: 611/ART, 30/ART, 322/ART and 422/ART, producing two types of offsets–1 (Average) and 2 (favors south bound); and two combinations in the evening: 311/ART and 433/NRT, yielding two kinds of offsets–1 (Aver-

age) and 3 (favors north bound). TRP pattern 30 appears to be a buffer plan for signal transitions and is not associated with an offset type number or a cycle length.

Table 4.2: Signal plan changes, evening traffic, 7/15/96

trans. time	CLEV	COFT	SPL/SF	ART/NRT	c.o.s	cycle (s)	offset
3:18 pm	4	A	1	ART	3.1.1	120	1
5:36 pm	4	A	1	NRT	4.3.3	134	3
6:31 pm	4	A	1	ART	3.1.1	120	1

Assuming that the local cycle starts at the beginning of mainline green, and the green time of the coordinated phase is the maximum green time allocated to that phase (we do not know the actual actuated split utilization), we sketched the time-space diagrams for the three intersections with various assumed traffic progression speeds (Figures 4.13–4.18). The cycles in these figures are normalized to 1 and all the parameters such as offsets, green time are expressed as percentages of a cycle.

The offset implemented during 6:00–6:36 am is derived from the COS 611/ART pattern. With an assumed progression speed of 65 mph, the green-bands for both south and north bound traffic are shown in Fig. 4.13. We can see from this figure that south bound traffic has a progression band of about 10 percent of the cycle, but north bound traffic has a very narrow progression band. Considering the traffic is heavier in the south bound direction, this offset clearly favors south bound traffic. Journey speeds during this period of time (Figs. 3.13 and 3.15) also confirm that this offset is adequate for good traffic progression in the south bound direction.

From 6:36 am to 7:22 am, there are two offsets used. One is derived from TRP pattern 30/ART , and the other from TRP pattern 322/ART. The first offset lasted only 2 minutes, which does not warrant a detailed examination. We sketched the time-space diagram for the second offset in Fig. 4.14 with an assumed progression speed of 55 mph. This offset is intended ensure a good progression for southbound traffic. The figure shows that south bound traffic has a progression band of about 10 percent of the cycle, but the progression band for north bound is virtually non-existent. Lydia to C2 has a maximum progression band for south bound traffic, which breaks at C, while C to C2 has a sizable progression band for north bound traffic, which breaks at Lydia. If we compare the progression bands at C2

and C with the journey speeds at these two links during this period (Figs. 3.13 and 3.15), we can see that wide progression band at C2 corresponds to high journey speeds for link Lydia to C2 while narrower progression band at C corresponds to lower journey speed for link C2 to C.

The offset made another transition at 7:22 am. This new offset, used till 8:46 am, is derived from pattern COS 422/ART. With an assumed progression speed of 45 mph (this is the default offset progression speed in the master controller), the progression bands are shown in Fig. 4.15. This offset is designed to provide maximum progression for peak south bound traffic. The actual progression from Lydia to C, however, is almost non-existent. To the contrary, it is the north bound traffic that enjoys good progression. This is not surprising if we consider the lane traffic distribution at C during the peak period. What happened here was that the lane closure downstrean of C led to long queues at C that broke the signal progression. It is clear that the progression band from Lydia to C2 is at its maximum. This good progression at C2 makes things worse for C: it discharges large amount of traffic to C. With one lane closed, C spent most of its time in the peak period to service queued-up vehicles (Fig. 4.15), leaving no room for good progression. This is clearly reflected in the low journey speeds on link C2 to C during this time period.

There are two offset changes from 8:46 to 9:00 am. One is transition from 422/ART to 322/ART, and the other from 322/ART to 30/ART. The first transition is rather brief. The second offset, derived from pattern 322/ART lasted about 12 minutes. With an assumed progression speed of 55 mph, the south bound progression band provided by the second offset is about 18 percent of the cycle length, while that for north bound is about 6 percent of the cycle length (Fig. 4.16). The good progression for south bound traffic in this case is interesting. This is partly due to the fact that south bound traffic demand around 9 am decreased to such a level that County Road C is no longer a bottleneck, thus the master controller was able to produce a good progression band for this demand level. This strongly suggests that the master controller does not have the capability of adaptively changing its timing plans to handle incident conditions.

In the evening periods, all offsets used provide no or very narrow progression band for south bound traffic (Figs. 4.17 and 4.18). As in the morning period, progression from Lydia to C2 is good, while from C2 to C is poor. This correlates strongly with the low journey speeds on link C2 to C throughout the evening period.

Figs. 4.19 to 4.29 give a general picture of the relationships between

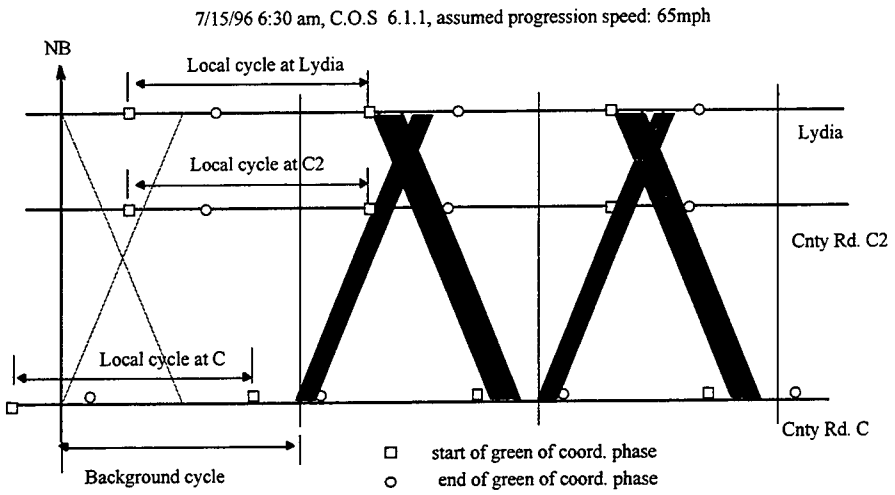

Figure 4.13: Signal offsets, 6:14–6:36 am

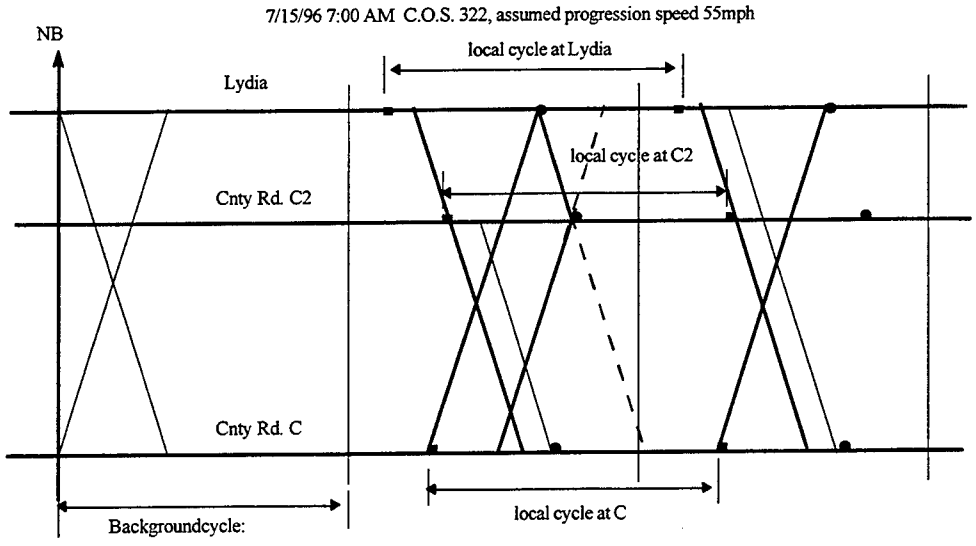

Figure 4.14: Signal offset, 6:38–7:22 am

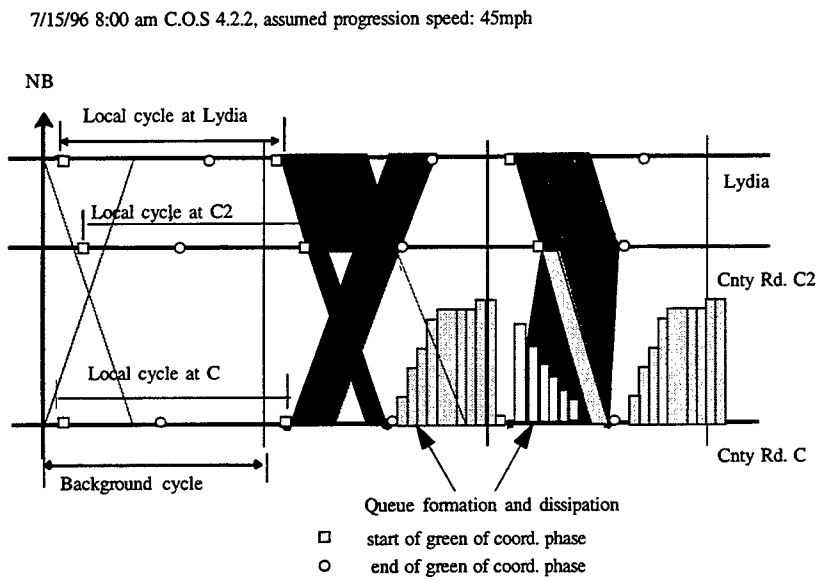

Figure 4.15: Signal offsets, 7:22–8:46 am

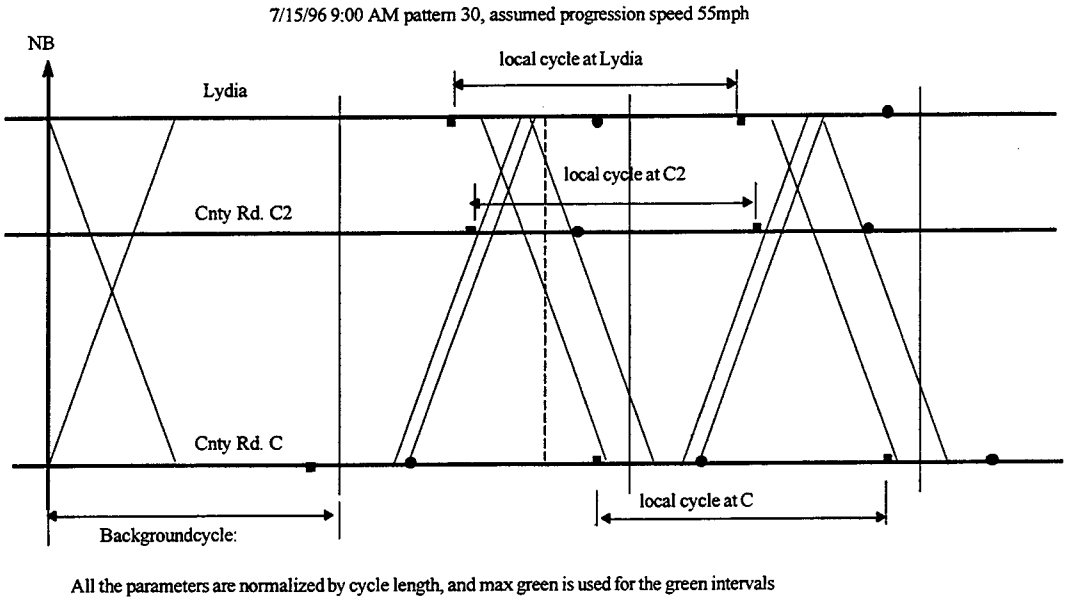

Figure 4.16: Signal offsets, 8:48–9:00 am

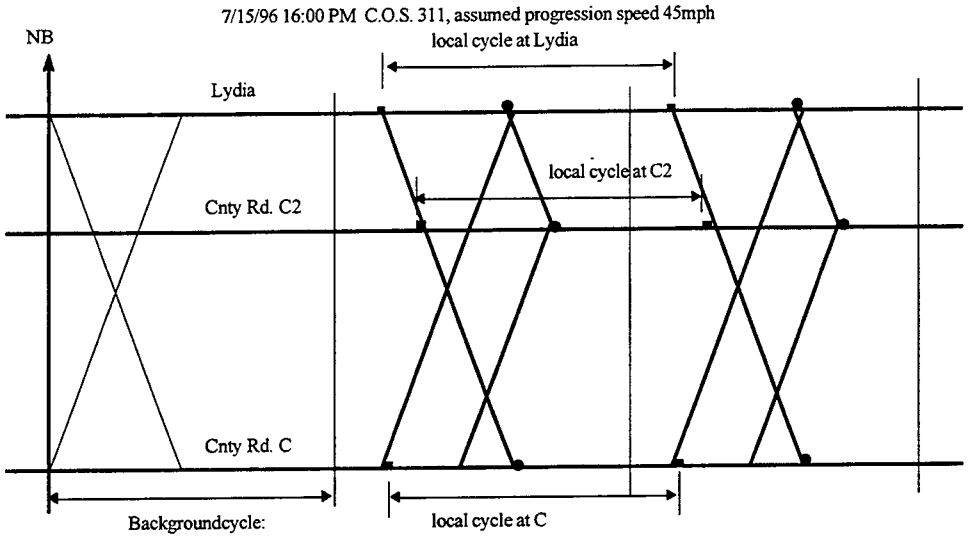

Figure 4.17: Signal offsets, 3:18–5:36 pm

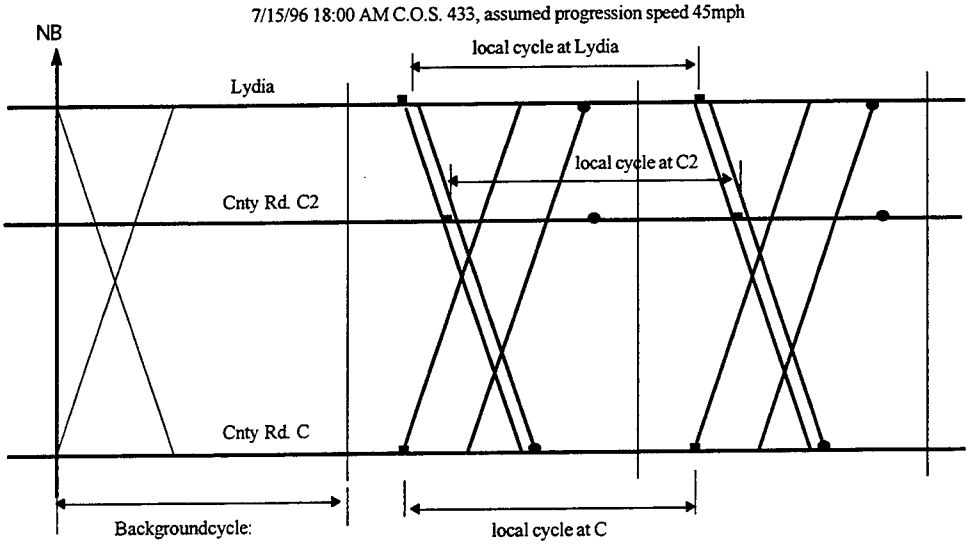

Figure 4.18: Signal offsets, 5:36–6:31 pm

journey speeds, v/c ratio (volume to capacity ratio), signal offset and occupancy for different C.O.S. values at the three intersections. Overall, wider greenband widths are associated with lower v/c ratio, smaller occupancy, and greater journey speeds. The dependence of journey speed on greenband width, however, is not one to one: any bandwidth that is greater than the minimum bandwidth required for good progression for a particular traffic pattern would yield roughly the same journey speeds.

Because the objective of any good control is to minmize traffic delay, one would observe high journey speeds under any demand patterns if the control is adequate. There are many occasions, however, existing control plans fail to handle a surge of demand or a reduction of road capacity, which often leads to a dramatic reduction of journey speeds. Our analyses in this chapter show that we can pick up clues from traffic paramters such as occupancy, v/c ratio and greenband width to tell if such events have occured in traffic.

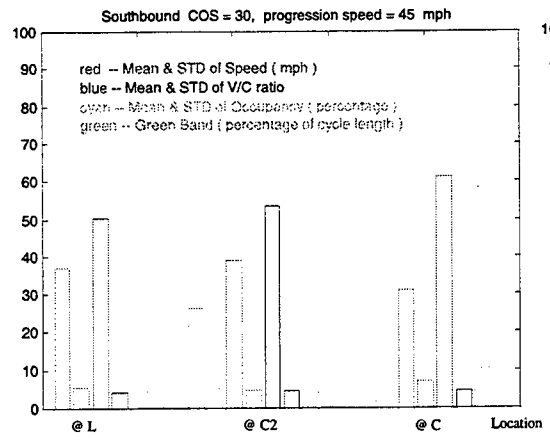

Figure 4.19: Journey speed, v/c ratio, occupancy and greenband width at COS 30

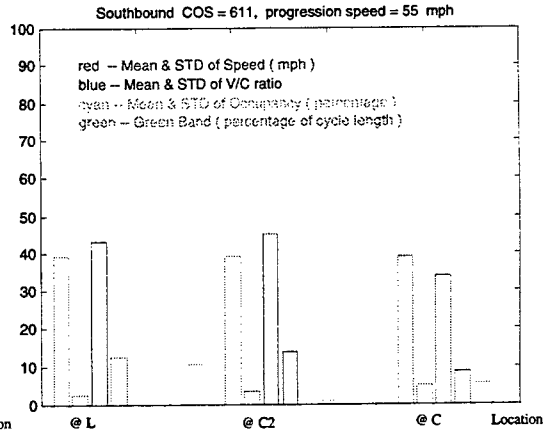

Figure 4.20: Journey speed, v/c ratio, occupancy and greenband width at COS 611

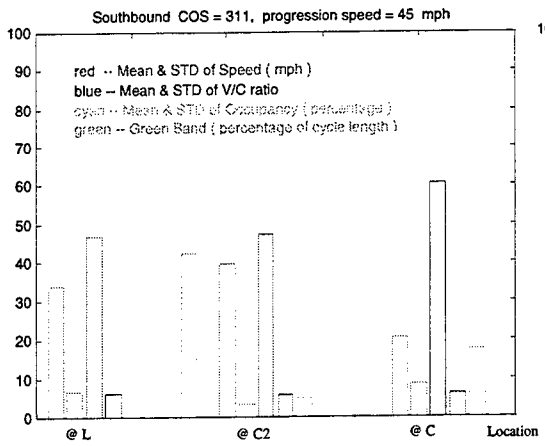

Figure 4.21: Journey speed, v/c ratio, occupancy and greenband width at COS 311

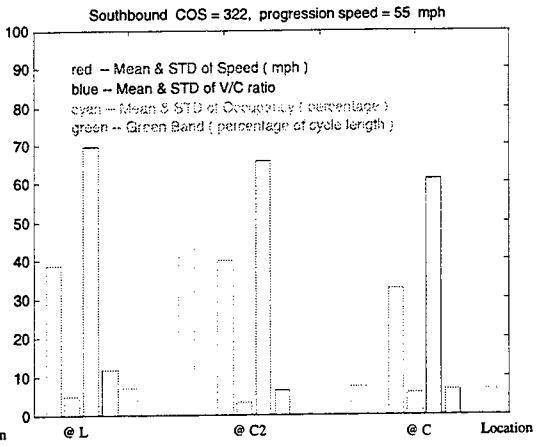

Figure 4.22: Journey speed, v/c ratio, occupancy and greenband width at COS 322

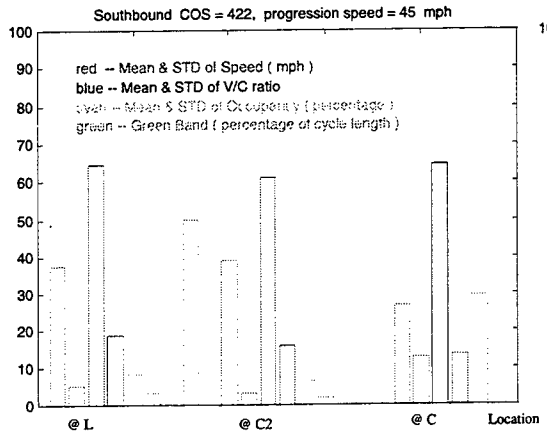

Figure 4.23: Journey speed, v/c ratio, occupancy and greenband width at COS 422

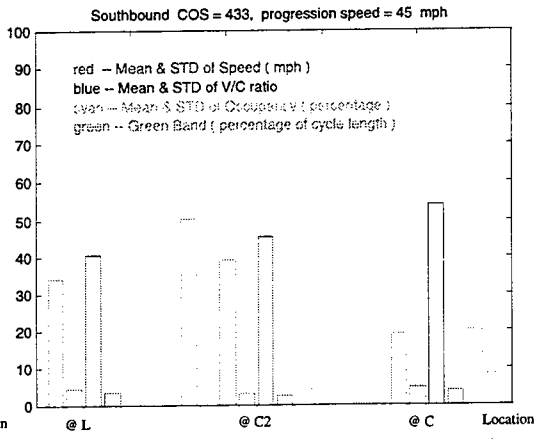

Figure 4.24: Journey speed, v/c ratio, occupancy and greenband width at COS 433

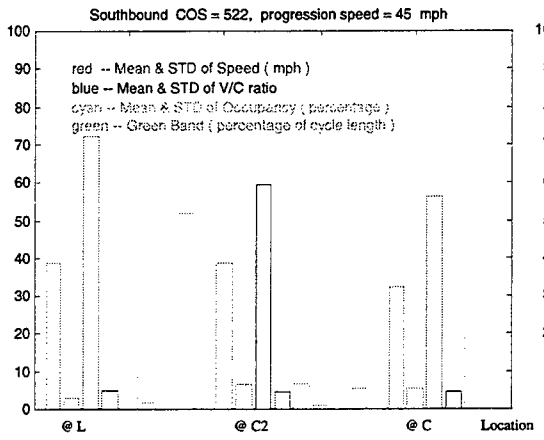

Figure 4.25: Journey speed, v/c ratio, occupancy and greenband width at COS 522

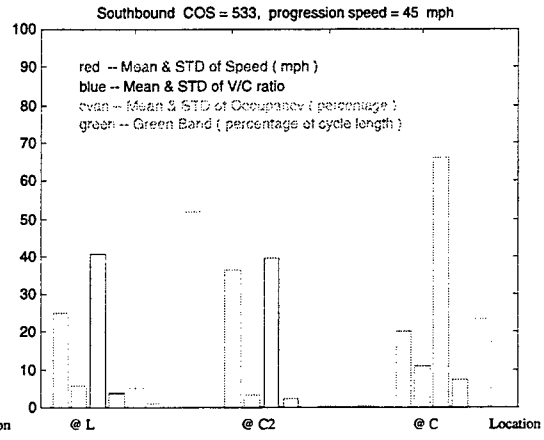

Figure 4.26: Journey speed, v/c ratio, occupancy and greenband width at COS 533

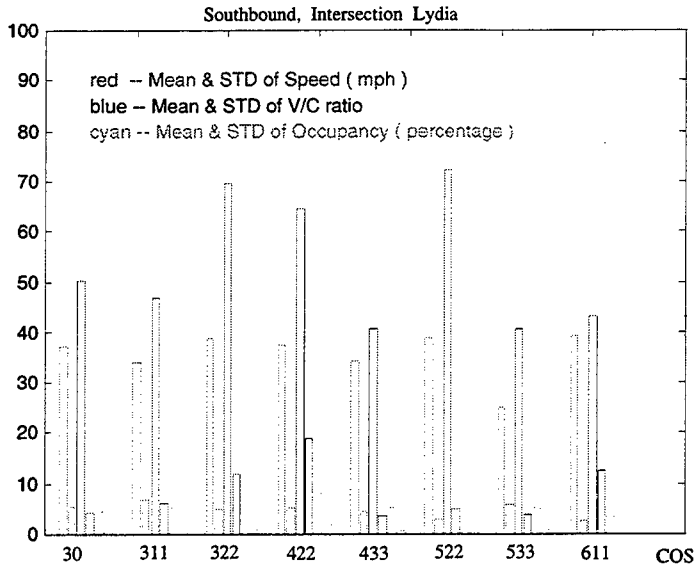

Figure 4.27: Journey speed, v/c ratio, and occupancy, Glenhill to Lydia

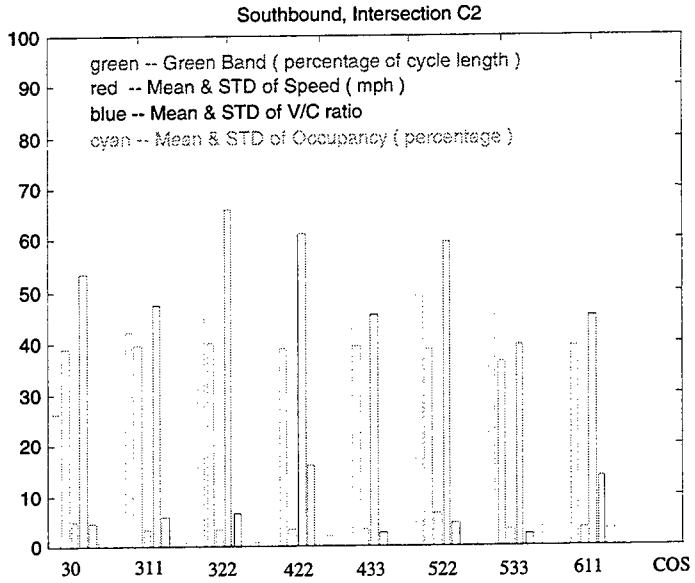

Figure 4.28: Journey speed, v/c ratio, and occupancy, Lydia to C2

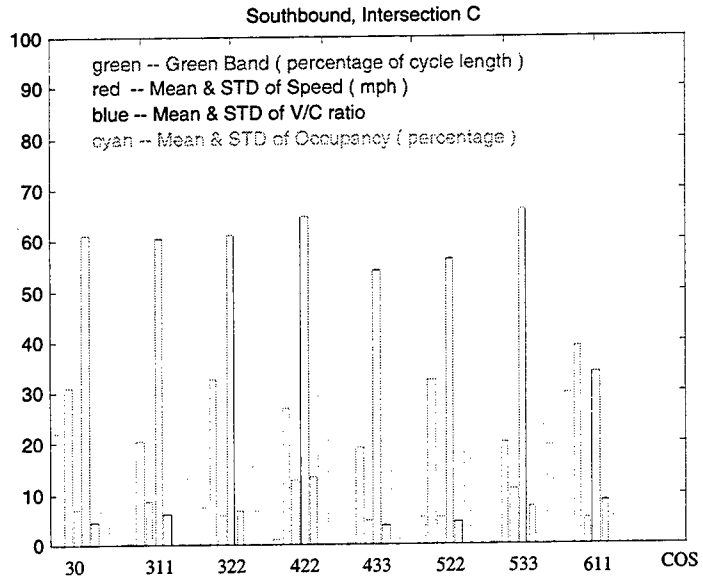

Figure 4.29: Journey speed, v/c ratio, and occupancy, C2 to C

Chapter 5

New journey speed models

This chapter describes the development of various arterial journey speed models. The analyses of Chapters 3 and 4 indicated that journey speed has rather stable patterns across weeks, week days and short time intervals if there are no incidents that disrupt these patterns, and that variations in journey speed cannot be fully explained by variations in flow patterns alone—links with similar flow patterns can have drastically different journey speeds. Other factors such as signal offset and/or greenband width and critical lane v/c ratio play an important role in explaining these speed variations. Furthermore, we found a strong correlation between journey speeds and spot speeds estimated from detector data under congested traffic conditions. Under light traffic conditions, spot speeds and journey speeds are uncorrelated, with spot speeds usually higher than journey speeds.

These findings provide strong clues to what should be included in an arterial journey speed estimation model. They do not, however, tell us what specific form should be adopted for the model. The selection of an appropriate model and the calibration of its parameters is subject to engineering judgment and experimentation. The remainder of this chapter describes the preliminary results in developing and evaluating an arterial journey speed model based on critical v/c ratio and estimated spot speeds.

5.1 Journey speed models

It has been shown in our previous analysis that critical v/c ratio, occupancy and greenband width[1] are the main factors that affect average link

[1]The width of a greenband is directly related to signal offset. Although greenband width has a sizable impact on intersection delay (therefore link journey speed), the limited

journey speeds. These factors are therefore natural candidate variables in an arterial journey speed model. Before determining model specifications, we first describe how some of these variables are computed from collected traffic data.

The journey speed of a link l is defined as

$$u_i = \frac{L}{t_i}$$

where L is the length of link l and t_i is the link travel time of the ith observation.

There are two ways to calculate mean journey speed. One is

$$\bar{u}_a = \frac{1}{n}\sum_i u_i$$

(the arithmetic mean), and the other is

$$\bar{u}_g = \frac{nL}{\sum_i t_i} \tag{5.1}$$

(the geometric mean).

The geometric mean is also called the space-mean speed in traffic engineering literature. In our calculations, the space-mean speed is used as the average journey speed ($u_a \geq u_g$).

The spot speed, derived from the relationship between traffic flow and concentration, is calculated from detector measurements:

$$u = \frac{q}{\rho} \tag{5.2}$$

where flow rate q is directly measured by a loop detector, and the concentration ρ is obtained from detector occupancy measurement o using

$$o = 100\overline{L}\rho \tag{5.3}$$

where $\overline{L}$ is the average effective vehicle length of the traffic stream that passed the detector during the sampling interval T. This length comprises two parts: vehicle length and loop detector length. Assuming an average of

number of changes in bandwith significantly reduces the prediction power of this input because a wide range of journey speeds exist for each bandwidth. Greenband width is therefore not used in the journey speed models.

14 feet for a vehicle and 6 feet for a loop detector, we have $\overline{L} = 20ft$. This would yield

$$o = 0.379\rho \tag{5.4}$$

Unlike journey speeds, which reflect travel conditions over an entire link in a time period, spot speeds measure travel conditions *near* the location of a detector.

Another quantity that needs to be calculated is critical v/c ratio. Suppose a link l has n through lanes, each with saturation flow rate $S_i, i = 1, \cdots, n$ and allocated green time $g_i, i = 1, \cdots, n$. The flow on lane i is q_i, and the cycle length at the downstream intersection of link l is C. The critical v/c ratio for link l is then:

$$\left(\frac{v}{c}\right)_{\text{critical}} = \max_{i=1,\cdots,n}\left(\frac{\frac{q_i}{S_i}}{\frac{g_i}{C}}\right) = \max_{i=1,\cdots,n}\left(\frac{q_i C}{S_i g_i}\right) \tag{5.5}$$

5.1.1 The data

A total of ten days of traffic data were collected for four links: two northbound links on Snelling Avenue (from County Road C to County Road C2 and from County Road C2 to Lydia) and two southbound links (from Lydia to County Road C2 and from County Road C2 to County Road C). The data collection periods in each day are 6:15 pm– 9:00 am and 15:45 pm–18:30 pm. These data were originally collected in five-minute intervals, then aggregated into 15-minute intervals for model-building. After aggregation, the total number of observations are reduced to

4(links) $\times$ 10(days/link) $\times$ 6(hours/day) $\times$ 4(data points/hour) = 960 data points

Each data point comprises average travel time, mean journey speed, occupancy, flow rate, offset, cycle length, green splits and so forth.

The 955[2] data points are then grouped into three data sets: the first set consists of data (averages) from the first five days (Data Set 1), the second set comprises data (averages) from the second five days (Data Set 2), and the third set consists of the averages of the entire ten days (Data Set 3). Next we use Data Sets 1–3 to calibrate and validate various journey speed models.

[2]There are five data points missing from the original observations.

5.1.2 The v/c ratio model

The analyses carried out earlier indicates that volume/capacity ratio strongly affects travel times, and therefore journey speeds. Our first attempt is therefore to develop a journey speed model based on critical v/c ratio.

Mean journey speeds and v/c ratios for the three data sets are shown in Figures 5.1–5.3. It can be seen from these figures that a nonlinear curve can be used to fit journey speed and v/c ratio data. The following function is selected:

$$\bar{u}_{\frac{v}{c}} = u_f - \alpha e^{\beta \frac{v}{c}} \tag{5.6}$$

where u_f, α and β are parameters to be determined by minimizing the differences between estimated mean journey speed $\bar{u}_{\frac{v}{c}}$ and observed mean journey speed $\bar{u}_g$.

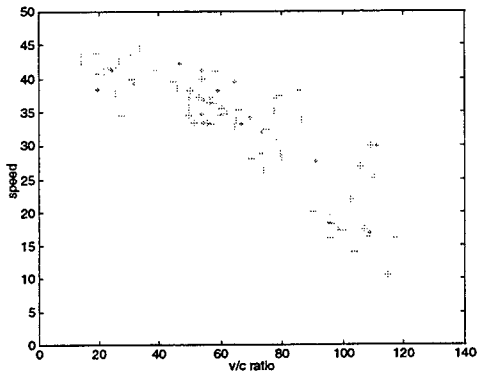

Figure 5.1: Data Set 1

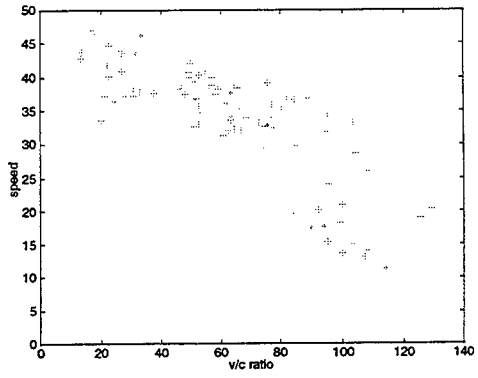

Figure 5.2: Data Set 2

The parameter values obtained through the curve-fitting of three data sets are listed in Table 1, and the resulting speed-v/c ratio curves are shown in Figures 5.4–5.6[3]. It should be noted that the parameter u_f describes the free flow speed on arterial streets, which is about 50 mph on the selected Snelling Avenue links.

5.1.3 The spot speed model

As v/c ratio increases to a certain critical point, the delay at an intersection becomes a major component of link travel time. One therefore would expect

[3][a,b,c] in Figures 5.4–5.6 correspond to $[\alpha, \beta, u_f]$ in the text.

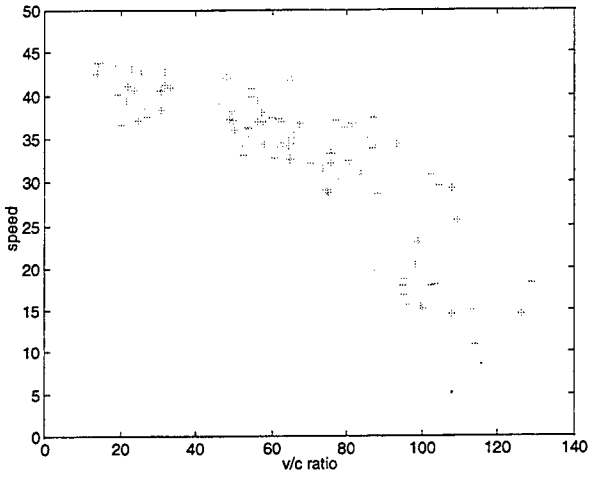

Figure 5.3: Data Set 3

Table 5.1: Estimated parameters of $\frac{v}{c}$ ratio models

model	cali. data	α	β	u_f
Model 1	Data Set 1	6.199	0.01431	49.74
Model 2	Data Set 2	7.119	0.01352	51.90
Model 3	Data Set 3	6.032	0.01462	49.94

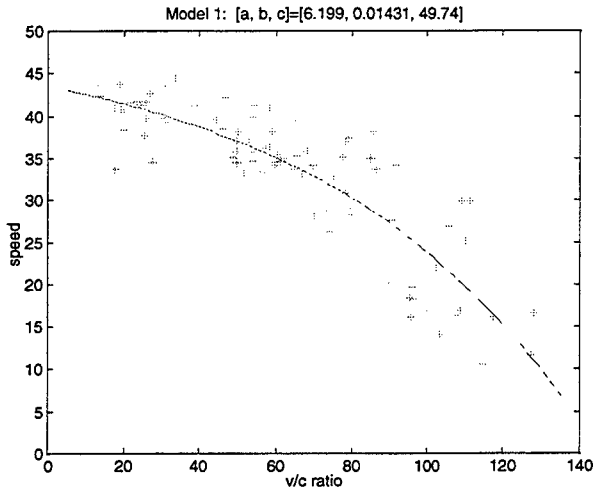

Figure 5.4: Curve-fitting using Data Set 1

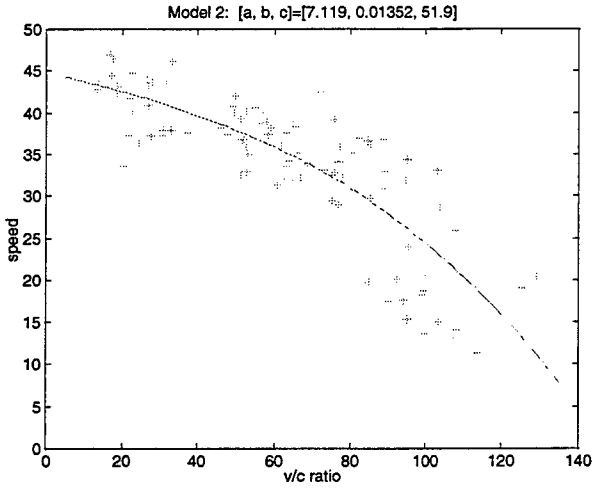

Figure 5.5: Curve-fitting using Data Set 2

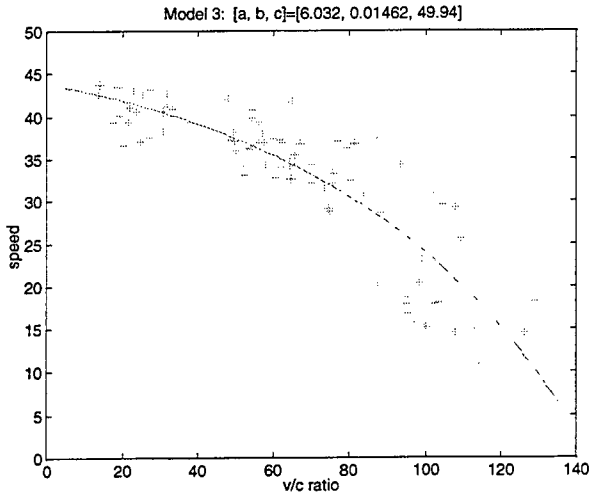

Figure 5.6: Curve-fitting using Data Set 3

that average speeds measured by a detector located near the intersection on a link largely determine the average journey speeds on that link. Figure 3.1 appears to confirm this hypothesis.

Rather than using Eq. 5.2 to calculate spot speeds for each time interval and average them afterwards, the following formula is used to calculate mean spot speeds for each time interval:

$$\bar{u}_{\underset{o}{q}} = 0.379 \frac{\sum_i q_i}{\sum_i o_i} \tag{5.7}$$

where i is the number of observations in each time interval.

The calculated average spot speeds and journey speeds are plotted in Figures 5.7–5.9. Spot speeds clearly overestimate journey speeds in light traffic, but closely match journey speeds in congested traffic when speeds are below 15 mph.

5.1.4 The combined model

To improve the reliability and accuracy of the estimated journey speeds, we combine the journey speed estimates from the v/c ratio model and the spot-speed model into a single estimate:

$$\bar{u}_c = \gamma \bar{u}_{\underset{c}{v}} + (1 - \gamma) \bar{u}_{\underset{o}{q}} \tag{5.8}$$

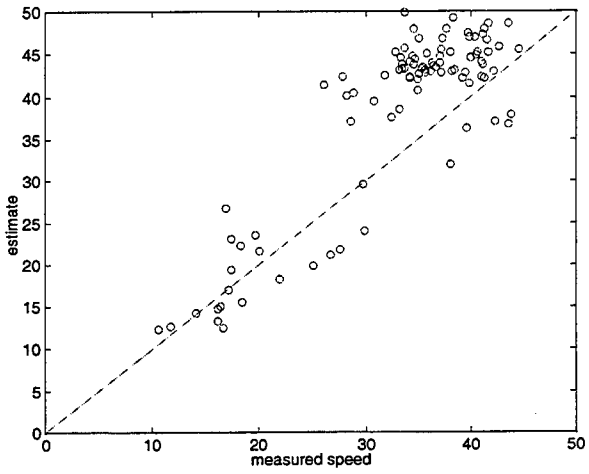

Figure 5.7: Spot speed vs. journey speed, Data Set 1

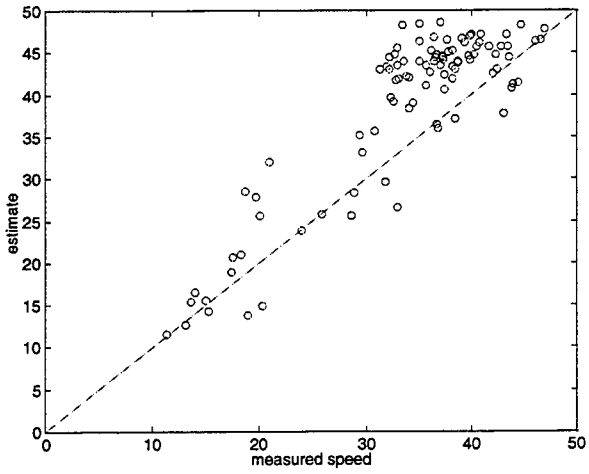

Figure 5.8: Spot speed vs. journey speed, Data Set 2

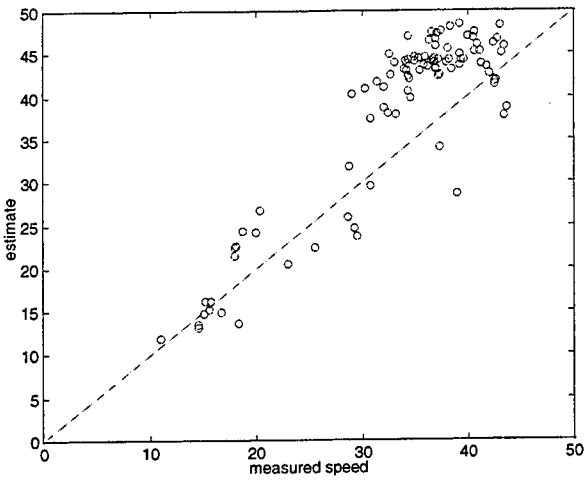

Figure 5.9: Spot speed vs. journey speed, Data Set 3

We can select from a number of choices for γ: we can choose $\gamma = 1$ for light traffic and $\gamma = 0$ for heavy traffic, or simply use $\gamma = \frac{1}{2}$. The latter represents the average of the two estimates and has been adopted in this project for its simplicity.

5.2 Model validation

We first evaluate the accuracy of the v/c ratio model. Remember that the v/c ratio for Model 1 was calibrated using Data Set 1, therefore we use Data Set 2 to evaluate Model 1. The result is shown in Figure 5.10. Similarly we use Data Set 1 to validate v/c ratio Model 2 and Data Set 3 to validate v/c ratio Model 3. The results are shown in Figures 5.11 and 5.12, respectively.

Estimated journey speeds above 30 mph are relatively accurate. The largest estimation error occurs in the 20–30 mph range, which is also true for journey speed estimates using flow and occupancy. This is not surprising if one considers that in this speed range traffic is typically in rapid transition—either from an uncongested regime to a congested regime or vice versa. Under such conditions, the delay part is not fully captured by either the detector information or the nominal signal timing parameters. More traffic information is needed to improve estimation accuracy in the transition region.

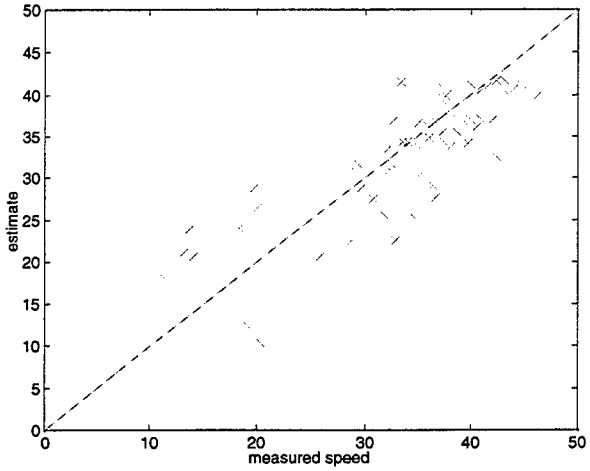

Figure 5.10: Testing Model 1 with Data Set 2

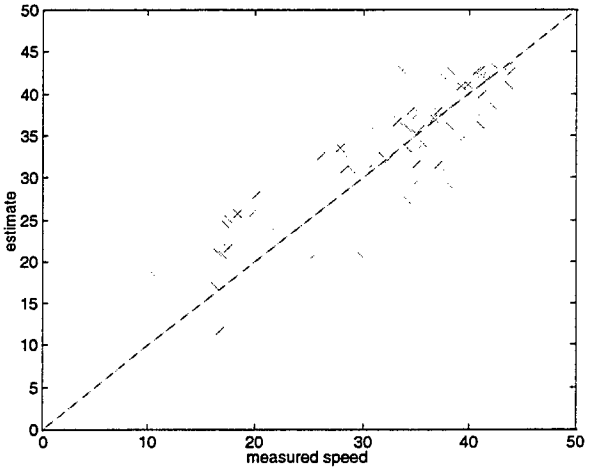

Figure 5.11: Testing Model 2 with Data Set 1

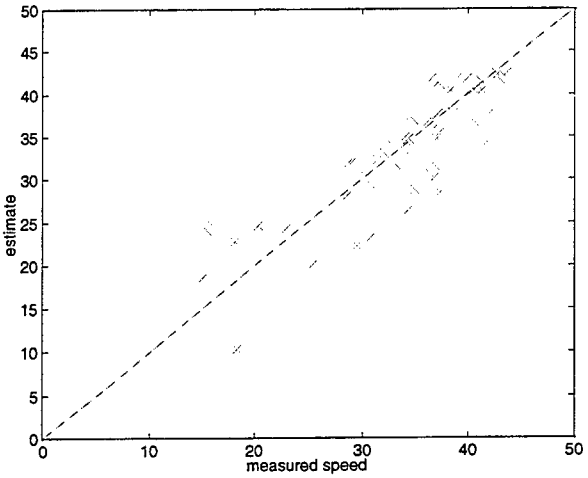

Figure 5.12: Testing Model 3 with Data Set 3

Next we validate the combined models using the three data sets. Figure 5.13 shows the results of evaluating Model A (which combines Model 2 and the spot speed model) using Data Set 1. Clearly this combined model is an improvement over the v/c ratio and spot speed models because the estimation errors of the two latter families of models tend to cancel each other. The validation results for two other combined models (Model B is a combination of Model 1 and the spot speed model; Model C is a combination of Model 3 and the spot speed model) are shown in Figures 5.14 and 5.15. They are nearly identical to Figure 5.13.

Although the models need to be significantly improved in the transition region, they appear to perform adequately for the first generation traveler information systems in which traffic conditions are divided into a number of ranges and are displayed on colored maps. For example, if we divide arterial journey speed into three ranges: [0,15], [15,30] and [30,45] (mph), the combined models can estimate average journey speed quite satisfactorily (See Figure 5.16 in which most of the data points fall within the shaded boxes).

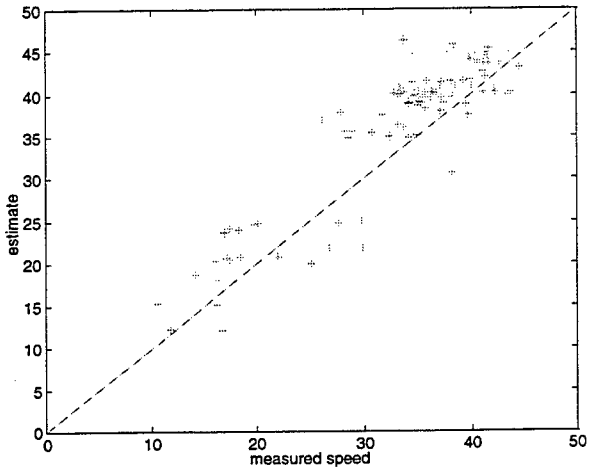

Figure 5.13: Testing combined Model A (Model 2 and spot speed) using Data Set 1

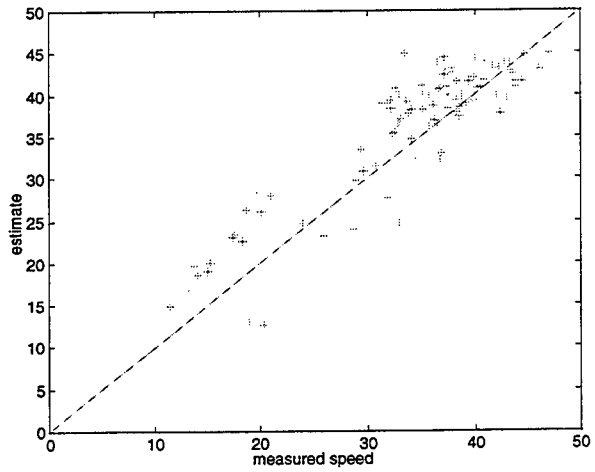

Figure 5.14: Testing combined Model B (Model 1 and spot speed) using Data Set 2

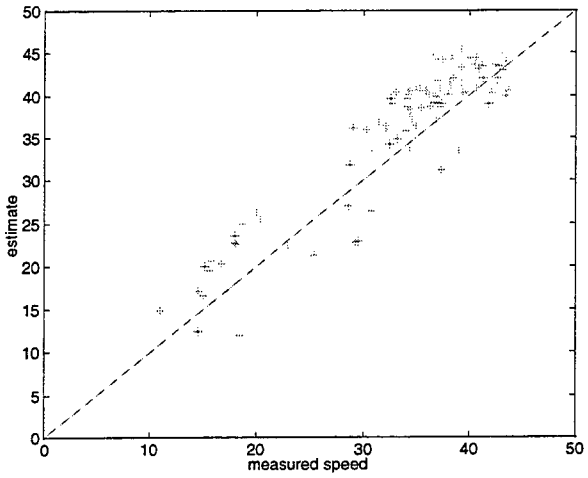

Figure 5.15: Testing combined Model C (Model 3 and spot speed) using Data Set 3

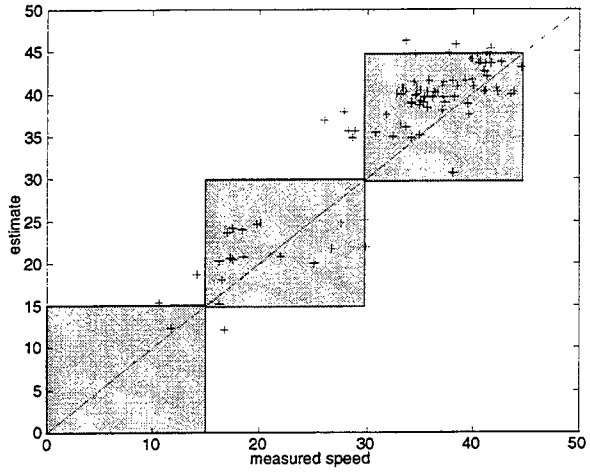

Figure 5.16: Estimation results by Model A

Chapter 6

Model Comparisons

This chapter compares the performance of the combined model (hereafter referred to as the *Iowa Model*) with a number of existing models, including the travel time models developed by Gault and Taylor (1981, hereafter referred to as the *British Model*) and by Sisiopiku and Rouphail (1994, hereafter referred to as the *Illinois Model*). The reasons that we choose these two models are 1) they are of the same type (regression) as the Iowa Model, 2) their inputs are readily available or computable from the MnLink data set and 3) they represent the state-of-the-art in the estimation of arterial travel times using loop data.

The functional forms for the three models are:

the British Model

$$\bar{t} = a\bar{o} + b \tag{6.1}$$

where $\bar{t}$ is the average link travel time. $\bar{o}$ is the average detector occupancy. a and b are parameters dependent on *undt* (undelayed travel time), x (degree of saturation) and *pdu* (downstream green ratio over upstream green ratio).

$$a = a_0 + a_1 \times undt + a_2 \times x + a_3 \times pdu \tag{6.2}$$

$$b = b_0 + b_1 \times undt + b_2 \times x + b_3 \times pdu \tag{6.3}$$

the Illinois Model

$$T = undt + delay \tag{6.4}$$

where T is link travel time, *delay* is determined by

$$delay = \beta_0 + \beta_1 \times detloc + \beta_2 \times o + \beta_3 \times grnrat \tag{6.5}$$

where *detloc* is the ratio of detector setback to link length, o is detector occupancy, *grnrat* is the green ratio (green time over cycle length). β_1, β_2, β_3, β_4 are regression parameters.

the Iowa Model

$$spd = \frac{1}{2}(spdv + spdo) \tag{6.6}$$

where

$$spdv = c - ae^{bx} \tag{6.7}$$

$$spdo = 0.379\frac{q}{o} \tag{6.8}$$

where a, b, c are parameters, x is degree of saturation, q is flow rate, o is detector occupancy.

6.1 Calibration procedure

These three models uses a variety of traffic parameters. Some parameters, such as occupancy and flow rate, are readily available from the data set, while some others, including green ratio and degree of saturation (v/c ratio), needs to be computed from other data in the data set. We shall list all the involved variables and their definitions, and for those that need to be computed from raw data, how they are calculated. First, the variable definitions:

- link travel time, T, in second
- undelayed link travel time, *undt*, in second
- detector occupancy, o, percentage
- degree of saturation, x
- downstream green ratio over upstream green ratio, *pdu*
- ratio of detector setback to link length, *detloc*
- green ratio, *grnrat*
- link flow rate, q, in veh/hr
- link travel speed, *spd*, in mi/hr

Next, the computation of certain variables:

- $undt = \frac{3600L}{5280V_f}$ where L is link length (feet), V_f is free flow speed (assumed to be 50 mi/hr)

- $x = \frac{q \times C}{S \times g}$ where C is cycle length, S is saturation flow rate (assumed to be 2000 veh/hr).

- $pdu = \frac{g_d}{g_u}$ where g_d and g_u are green time of downstream and upstream intersections respectively

- $grnrat = \frac{g}{C}$ where g is downstream intersection green time and C cycle length.

To perform both calibration and comparison of the selected models, we divide the traffic data for northbound links C–C2, C2–L and southbound links L–C2, C2–C into two subsets: subset one (Data Set 1) contains the data collected in the first five days and subset two (Data Set 2) contains the data collected in the next five days. For each link, data collected in the same 15-minute time interval on different days are averaged within each subset. The average journey speed on each link is then calculated

$$spd_i = \frac{3600L_i}{5280\bar{T}_i}$$

where $\bar{T}_i$ is the five-day average of link travel times on link i.

Finally, the least squares procedure is used to obtain the parameters for the three models. The error to be minimized is

$$\text{error} = \sqrt{\frac{1}{n}\sum_{i=1}^{n}(spd_i - \hat{spd}_i)^2} \tag{6.9}$$

where $\hat{spd}_i$ is the estimated speed.

The obtained parameters and the residual errors are listed in Tables 6.1 and 6.2.

6.2 Comparisons

It is clear from the calibration results that among the three models, the Iowa Model has the minimal residual errors. The British model has slightly

Table 6.1: Calibrated parameters of the three models using Data Set 1

Models	parameters	errors
British Model	$[a_0, a_1, a_2, a_3]$=[5.62, 0.0659, -1.04, -6.33] $[b_0, b_1, b_2, b_3]$=[-29.90, 1.17, 18.46, 24.49]	4.57
Illinois Model	$[\beta_0, \beta_1, \beta_2, \beta_3]$=[32.22, -37.48, 2.11, -46.79]	7.04
Iowa Model	[a, b, c]=[6.50, 1.40, 49.98]	4.02

Table 6.2: Calibrated parameters of the three models using Data Set 2

Models	parameters	errors
British Model	$[a_0, a_1, a_2, a_3]$=[6.85, 0.1089, -3.47, -6.58] $[b_0, b_1, b_2, b_3]$=[-24.18, 1.107, 21.53, 16.75]	5.51
Illinois Model	$[\beta_0, \beta_1, \beta_2, \beta_3]$=[40.44, -40.20, 1.98, -62.79]	9.43
Iowa Model	[a, b, c]=[7.77, 1.29, 52.57]	4.46

higher errors than the Iowa Model and the Illinois Model has the largest errors among the three models. The average errors, however, may not depict an accurate picture of how these models perform. We therefore plotted the predictions made by these models against measured data. Figs. 6.1 and 6.2 shows the respective predictions by the British and Illinois models (whose parameters are calibrated using Data Set 1) of average link travel times as compared to measured ones from Data Set 2. It appears that the British Model performs slightly better than the Illinois Model when travel times are either short or long. After converting link travel times into journey speeds, the journey speed predictions by the three models are compared (Figs. 6.3 and 6.4, 6.5 and 6.6). The figures show that all three models perform roughly the same at low journey speeds, but the Iowa Model outperforms the British Model and the Illinois Model at high speeds.

Figs. 6.7 – 6.12 shows the comparison results using Data Set 1 (the models are calibrated with Data Set 2). Similar conclusions can be drawn from these results.

Although the Iowa Model performs only slightly better than the other two models, it has a simpler model structure, fewer inputs, and more easily obtainable and interpretable parameters. The Iowa Model is developed based on traffic flow principles and a careful analysis of empirical data. Therefore it is expected that this model would be more transferable to other locations, a conjecture that can only be proved when traffic data from other

locations are available.

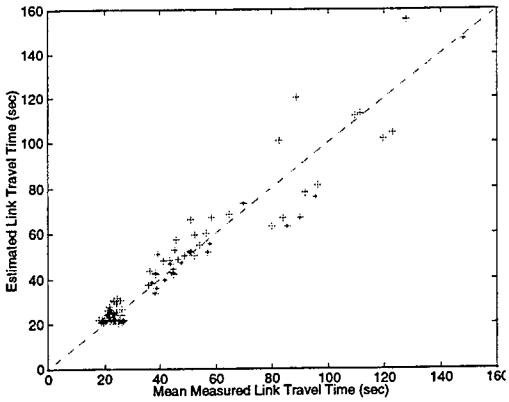

Figure 6.1: Estimates of Link Travel Times, the British Model, Data Set 2

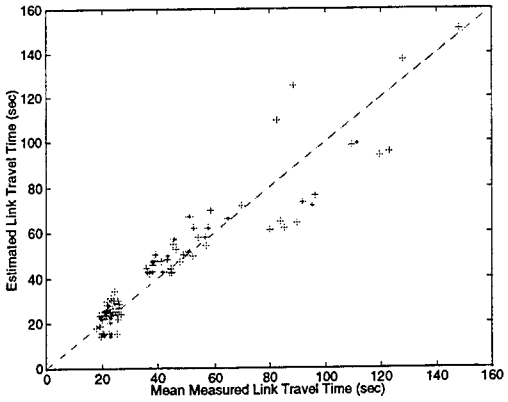

Figure 6.2: Estimates of Link Travel Times, the Illinois Model, Data Set 2

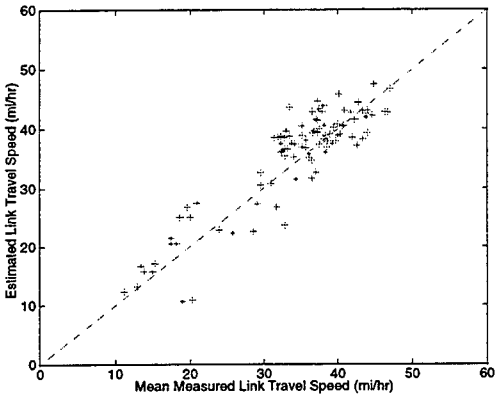

Figure 6.3: Est. vs. measured speed, the Iowa Model, Data Set 2

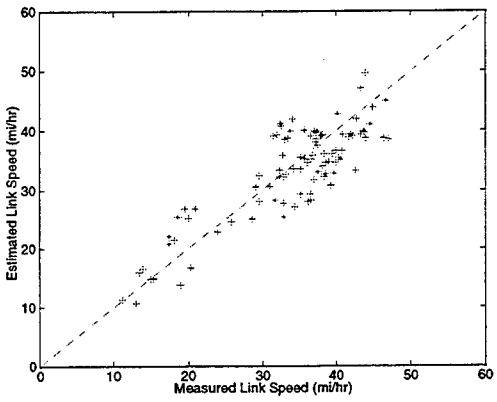

Figure 6.4: Est. vs. measured speed, the British Model, Data Set 2

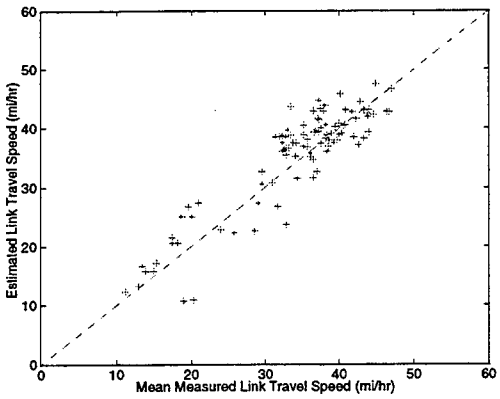

Figure 6.5: Est. vs. measured speed, the Iowa Model, Data Set 2

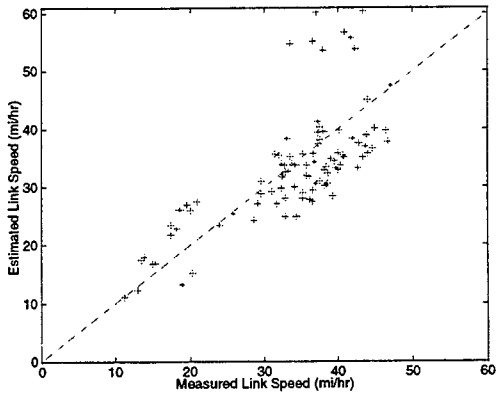

Figure 6.6: Est. vs. measured speed, the Illinois Model, Data Set 2

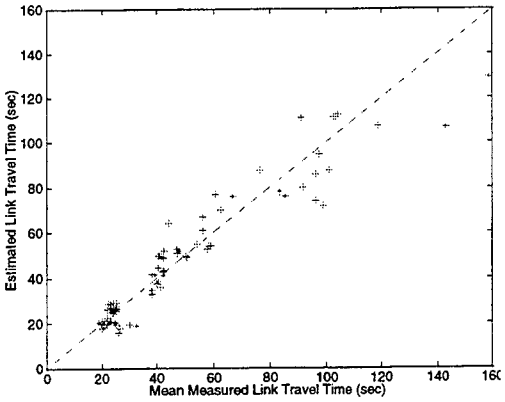

Figure 6.7: Estimates of Link Travel Times, the British Model, Data Set 1

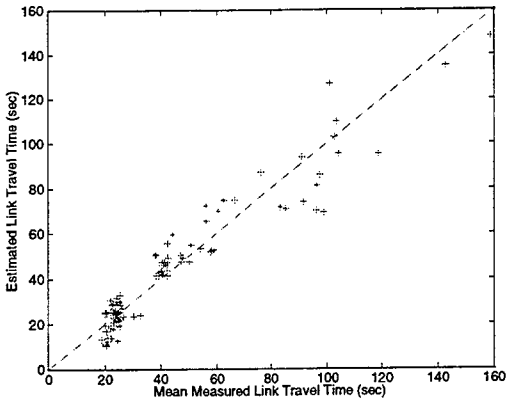

Figure 6.8: Estimates of Link Travel Times, the Illinois Model, Data Set 1

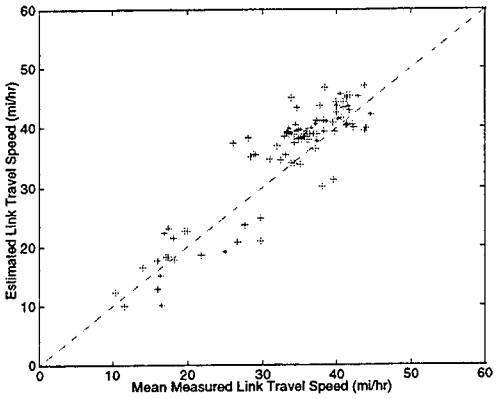

Figure 6.9: Est. vs. measured speed, the Iowa Model, Data Set 1

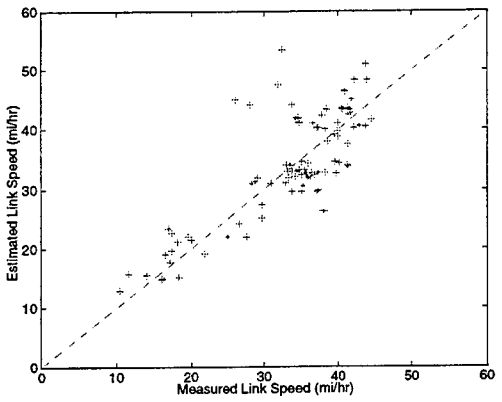

Figure 6.10: Est. vs. measured speed, the British Model, Data Set 1

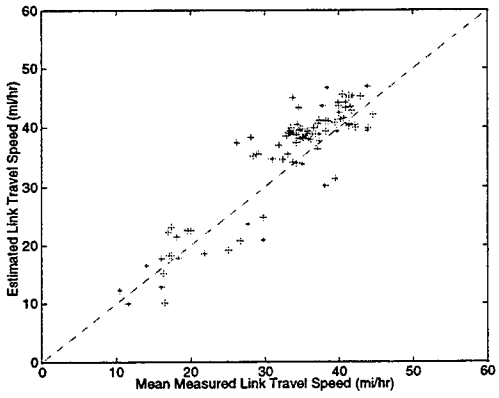

Figure 6.11: Est. vs. measured speed, the Iowa Model, Data Set 1

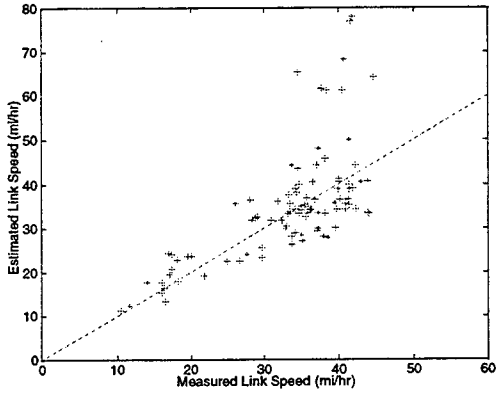

Figure 6.12: Est. vs. measured speed, the Illinois Model, Data Set 1

Chapter 7

Summary

This report describes the results obtained from Phase II of the travel time estimation project, which include analyses of traffic data, identification of factors that affect travel times, development and validation of journey speed models and comparison of a number of arterial travel time/journey speed models.

Our analysis centers on a new transformed variable, journey speed, rather than on travel time itself. We found that journey speeds have a strong correlation with spot speeds estimated from detector data in congested traffic conditions. This relationship, however, is nonlinear. At light traffic conditions, spot speeds and journey speeds are uncorrelated, with spot speeds usually higher than journey speeds. Because we are primarily interested in predicting travel times at congested conditions, the relationship between spot speeds and journey speeds can be utilized, together with other traffic information, to predict travel times for congested traffic.

We also studied both journey speed and traffic flow patterns for various time intervals. It is found that journey speed has rather stable patterns across weeks, week days and short time intervals. If no special events occur, these stable patterns can serve as the base predictor when real time traffic information is not readily available.

Our analyses also show that the variations of journey speeds are not fully explainable by variations in flow patterns alone. Links with same flow patterns can have drastically different journey speeds. This led us to derive some new traffic flow parameters, such as lane traffic distribution, and calculate certain signal timing parameters, such as greenband width, for explaining the journey speed variations. We found that the maximum per lane demand for the congested link is in fact much higher than that of

the uncongested link because of unbalanced lane traffic distribution, and the progression provided for the congested link is much poorer than that for the uncongested link.

Based on these analyses, we have developed three arterial journey speed models: the v/c ratio model, the spot speed model and the combined model. The v/c ratio model generally performs better at high journey speeds, the spot speed model performs better at low journey speeds, and the combined model performs reasonably well in both low and high journey speed ranges. All three models appear to have difficulty in accurately estimating journey speeds when traffic is in quick transition. The primary reason for this inability is that in this transition region journey speed is too sensitive to v/c ratio changes but spot speed is too insensitive to changes in delay[1]. Despite this weakness, the combined model yields acceptable journey speed estimates for the first generation advanced traveler information systems, in which ranges of journey speeds/travel times are provided to both travelers and system operators.

With the developed arterial journey speed models, Mn/DOT will be able to display real-time traffic flow conditions for both freeways and major arterial streets. Currently, Mn/DOT displays three levels of freeway traffic conditions based on estimated traffic speed: a link is red if its estimated speed is 20 mph or below, yellow if the estimated speed is 20–35 mph, and green if the estimated speed is 35 mph or above. For arterial streets, a similar pattern can be used: red for speeds below 15 mph, yellow for speeds between 15 mph and 30 mph, and green for speeds higher than 30 mph. The 5 mph difference between the same color displays for freeways and arterials is reasonable because drivers usually have higher expectations for freeways.

Although the accuracy of the developed arterial journey speed models are adequate for the purpose of displaying traffic conditions on colored maps, there are a number of issues that warrant further investigation. One issue is how to improve the performance of the model in the transition region of traffic flow. Attempts have been made to decompose travel time into two parts: running time and delay time, such that each part can be estimated more accurately. Because it is difficult to estimate the delay component with the collected data, however, the anticipated improvements were not realized.

Still, this does not invalidate the proposed approach, which we will re-

[1]Because system detectors are set back about 450 ft from the stopline, the speeds they register are relatively constant before queues grow near their locations. Journey speeds, on the other hand, have been significantly reduced due to queuing delays not reflected in detector data.

visit when data are collected in shorter time intervals (e.g., per signal cycle) by the Orion project. Another issue concerns the estimation of journey speeds under incident conditions. Currently we use the critical v/c ratio to capture, to a certain degree, the effects of lane-blocking incidents. This approach appears to perform well in modeling the lane closure downstream of the Snelling/County Road C intersection, but needs further validation and enhancement for other incident situations. Yet another issue is the aggregation of link journey speeds into section journey speeds (sections comprise a number of consecutive links), which involves two tasks: 1) grouping links into sections, and 2) obtaining section journey speeds from link journey speeds. The first task can easily be performed by an experienced traffic engineer. The second task, on the other hand, needs more investigation because there are a number of ways to perform this task but it is not obvious which one is the most appropriate.

The set of models developed by this project have undergone only limited evaluation. Further validation for a variety of traffic flow conditions and road geometries will be necessary before these models can be widely deployed. We plan to work closely with Mn/DOT traffic engineers and the Orion project team to continuously improve and modify these models during their field testing and implementation; we will address some of the unresolved issues in our further work for the Minnesota Department of Transportation. We hope that our work will make worthwhile contributions to Mn/DOT's ongoing effort to stay ahead of traffic gridlock through progressive transportation management schemes such as advanced traveler information systems.

References

1. Gault, H. E., and I. G. Taylor, "The Use of the Output from Vehicle Detectors to Assess Delay in Computer-Controlled Area Traffic Control Systems," Research Report 31. Transport Operation Research Group, University of Newcastle upon Tyne, England, 1981.

2. Gipps, P. G., "The Estimation of a Measure of Vehicle Delay from Detector Output". Research Report 25. Transport Operation Research Group, University of Newcastle upon Tyne, England, 1977.

3. Sisiopiku, Virginia and Rouphail, Nagui, "Travel Time Estimation from Loop Detector Data for Advanced Traveler Information Systems Applications," Technical Report, Illinois University Transportation Research Consortium. June 1994.

4. Takaba, S., T. Morita, and T. Hada, "Estimation and Measurement of Travel Time by Vehicle Detectors and License Plate Readers," Proc., Vehicle Navigation and Information Systems Conference, Vol. 1, Society of Automotive Engineers. 1991, pp. 257267.

5. Young, C. P., "A Relationship Between Vehicle Detector Occupancy and Delay at Signal-Controlled Junctions, Traffic Engineering and Control, Vol. 29, 1988 pp. 131134.

6. Zhang, H. M., Wu, T., Kwon, E., Sommers, K. and A. Habib, "Arterial link travel time estimation using loop detector data," Technical Report to U.S. Department of Transportation and Minnesota Department of Transportation, May 1997.